



Kavli Institute for  
Theoretical Physics

University of California, Santa Barbara

Quantifying and Understanding the  
Galaxy — Halo Connection

May 15-19, 2017

**Structural Evolution in the Galaxy-Halo Connection,  
and Halo Properties as a Function of  
Environment Density and Web Location**

**Joel Primack**

**UCSC**

with collaborators including Aldo Rodriguez-Puebla, Christoph Lee, Peter Behroozi, Sandy Faber, Radu Dragomir, Tze Ping Goh, Miguel Aragon Calvo, Doug Hellinger, Anatoly Klypin, Viraj Pandya, Rachel Somerville, & Avishai Dekel



Kavli Institute for  
Theoretical Physics  
University of California, Santa Barbara

Quantifying and Understanding the  
Galaxy — Halo Connection

May 15-19, 2017

# Structural Evolution in the Galaxy-Halo Connection, and Halo Properties as a Function of Environment Density and Web Location

Joel Primack

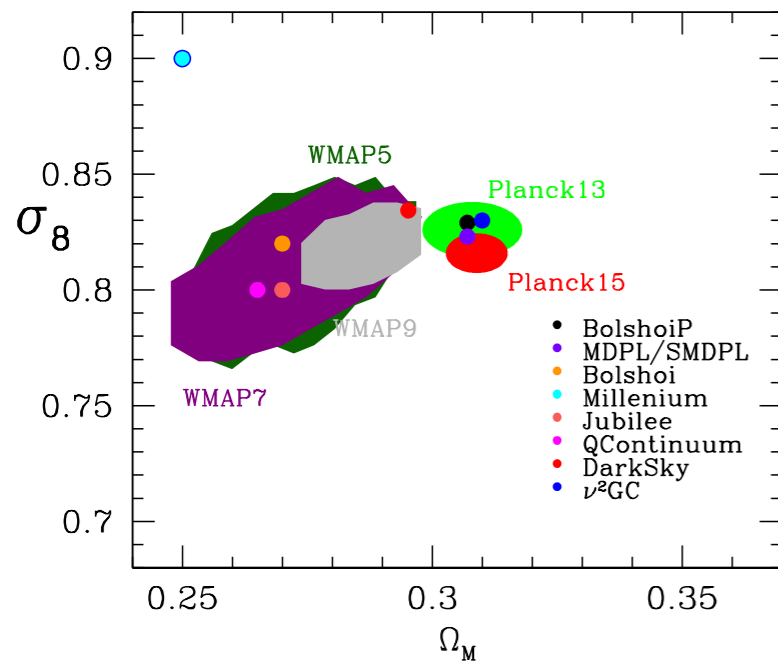
- **SHARC**:  $\sim 0.3$  dex dispersion in halo  $\dot{M}/M \Rightarrow$  similar dispersion in  $\dot{M}^*/M^*$  on the Main Sequence
- **Abundance matching with radii & mergers**  $\Rightarrow R^* \sim M^{1/3}$  goes to  $R^* \sim M^{2/3}$  after quenching, & **quenching downsizing**:  $\Sigma_1$  grows till quenching,  $\Sigma_{1,\text{quench}}$  larger & at higher  $z$  for higher  $M^*$
- **Galaxy 3D half-mass radii**  $R_{3D}^* \approx 0.5 \langle \lambda_{\text{Bullock}} \rangle R_{\text{halo}}$  for  $0 < z < 3$ , but  $\langle \lambda_{\text{Peebles}} \rangle \downarrow$  with  $z \uparrow$
- **Halo properties**  $\dot{M}/M$ ,  $\lambda$ ,  $C_{\text{NFW}}$ ,  $a_{\text{LMM}}$ , **shape don't depend on web location at fixed density**
- **Spin  $\lambda$  30% smaller at low density tests whether galaxy  $R^*$  is determined by host halo  $\lambda$**
- **Halo Mass Loss: Evaporation after Merger**  $\Rightarrow C_{\text{NFW}} \downarrow$  &  $\lambda \uparrow$ , **Tidal Stripping**  $\Rightarrow C_{\text{NFW}} \uparrow$  &  $\lambda \downarrow$
- **Galaxy Luminosity-Halo Mass, Stellar Mass-Halo Mass relations are independent of density**
- **Forming galaxies are elongated & oriented along filaments, become round after compaction**

# Halo and Subhalo Demographics with Planck Cosmological Parameters: Bolshoi-Planck and MultiDark-Planck Simulations

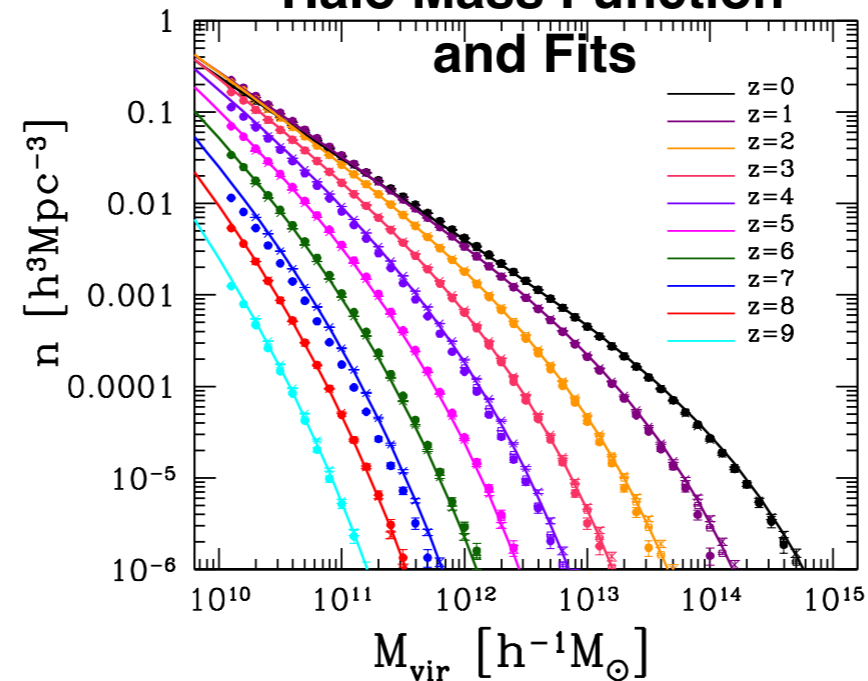
Aldo Rodríguez-Puebla, Peter Behroozi, Joel Primack, Anatoly Klypin, Christoph Lee, Doug Hellinger

MNRAS 2016

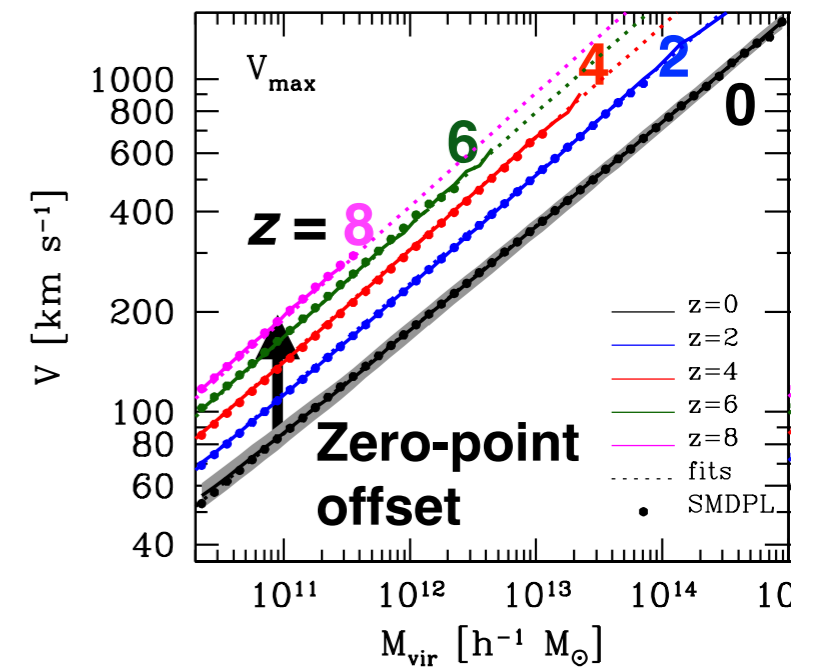
## Cosmological Simulations



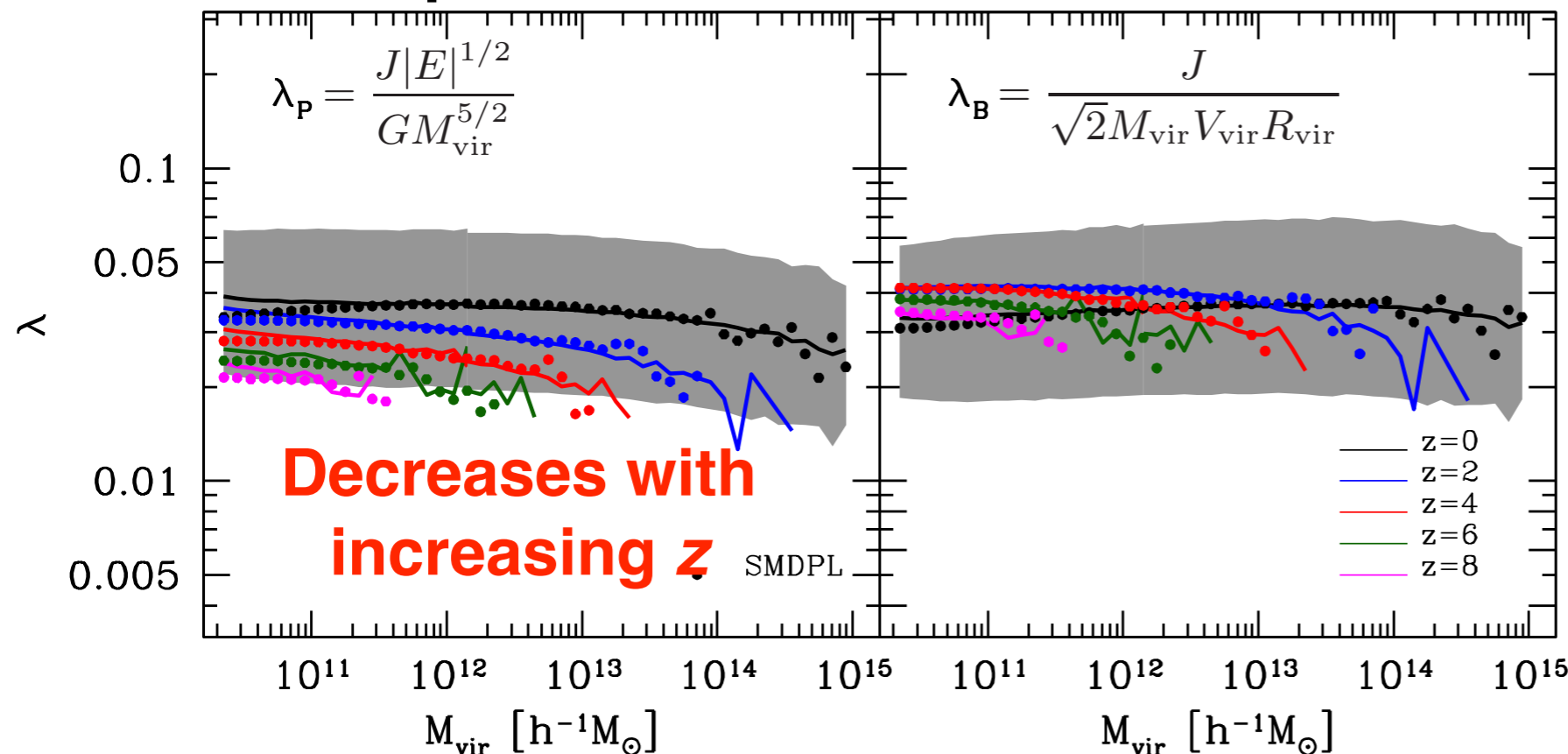
## Halo Mass Function and Fits



## $V_{\text{max}}(M_{\text{vir}}, z)$



## Halo Spin Parameters as a function of $M_{\text{vir}}$



*We have now released the halo catalogs and merger trees from Bolshoi-Planck and MultiDark-Planck cosmological simulations. Our paper includes Appendices with instructions for reading these files.*

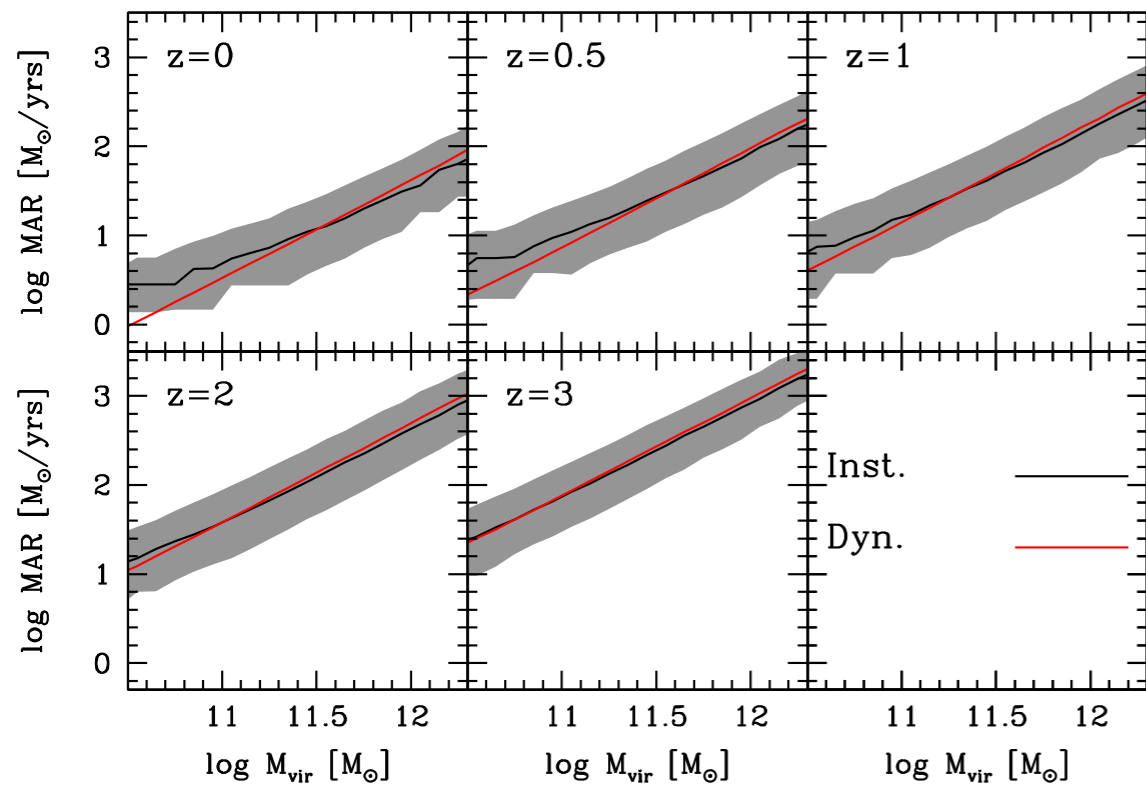
<http://hipacc.ucsc.edu/Bolshoi/MergerTrees.html>

Medians are shown as the solid lines. At  $z = 0$  the grey area is the 68% range.

# Is Main Sequence SFR Controlled by Halo Mass Accretion?

by Aldo Rodríguez-Puebla, Joel Primack, Peter Behroozi, Sandra Faber **MNRAS 2016**

## Halo mass accretion rates z=0 to 3



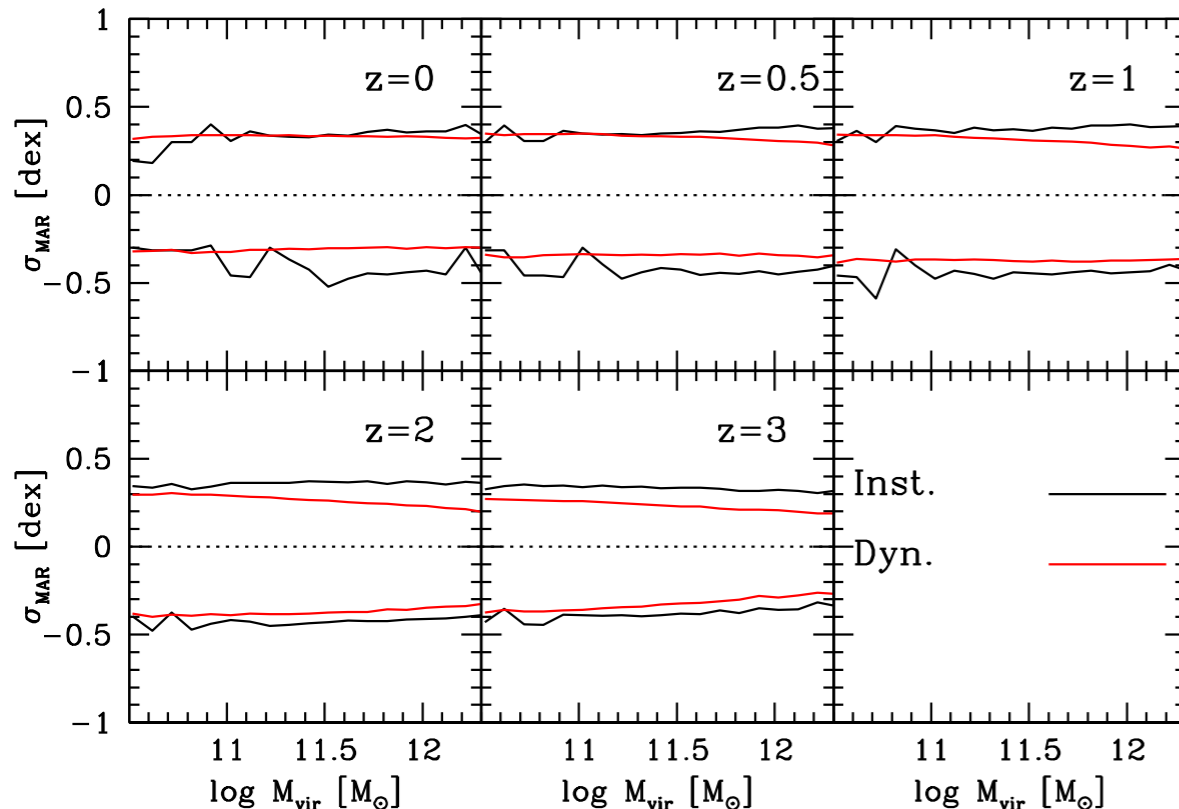
$$\frac{dM_*}{dt} = \frac{\partial M_*(M_{\text{vir}}(t), z)}{\partial M_{\text{vir}}} \frac{dM_{\text{vir}}}{dt} + \frac{\partial M_*(M_{\text{vir}}(t), z)}{\partial z} \frac{dz}{dt}$$

but if the  $M_*-M_{\text{vir}}$  relation is **independent of redshift** then the stellar mass of a central galaxy formed in a halo of mass  $M_{\text{vir}}(t)$  is  $M_* = M_*(M_{\text{vir}}(t))$ . From this relation star formation rates are given simply by

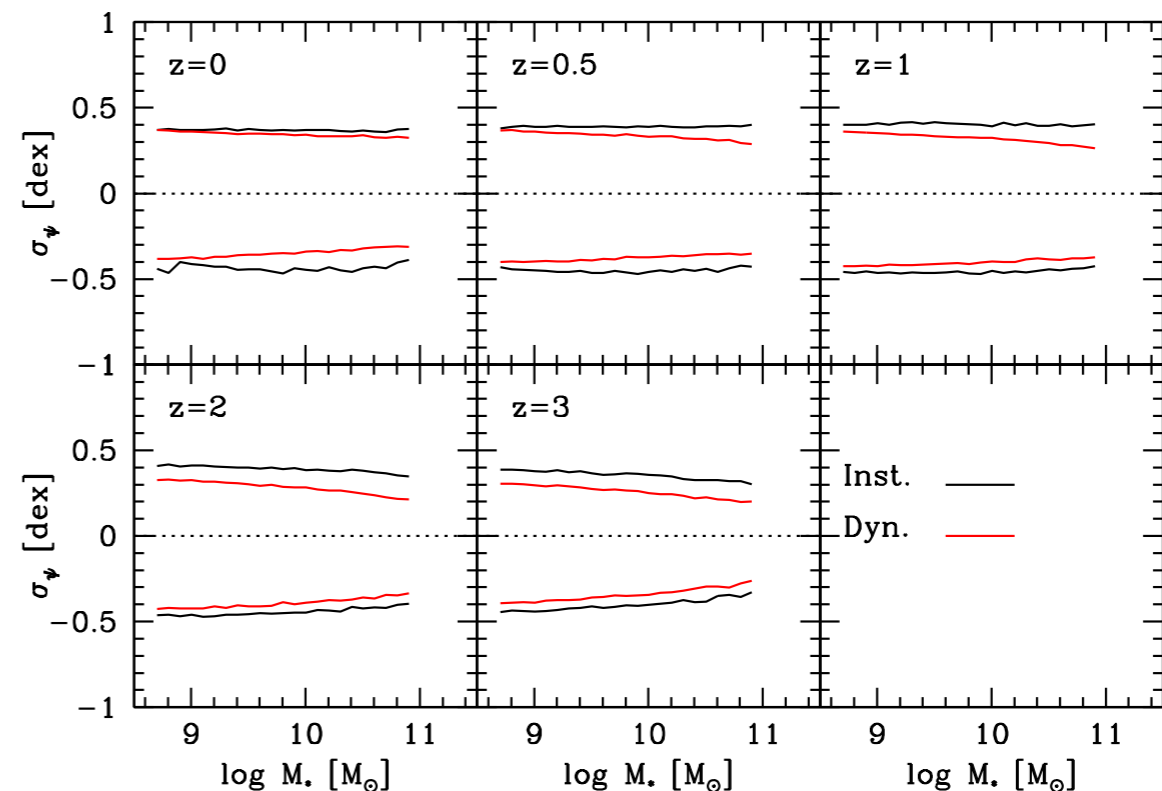
$$\frac{dM_*}{dt} = \frac{\partial M_*(M_{\text{vir}}(t), z)}{\partial M_{\text{vir}}} \frac{dM_{\text{vir}}}{dt} = f_* \frac{d \log M_*}{d \log M_{\text{vir}}} \frac{dM_{\text{vir}}}{dt},$$

where  $f_* = M_*/M_{\text{vir}}$ . We call this **Stellar-Halo Accretion Rate Coevolution (SHARC)** if true **halo-by-halo for star-forming galaxies**.

## Scatter of halo mass accretion rates



## Implied scatter of star formation rates



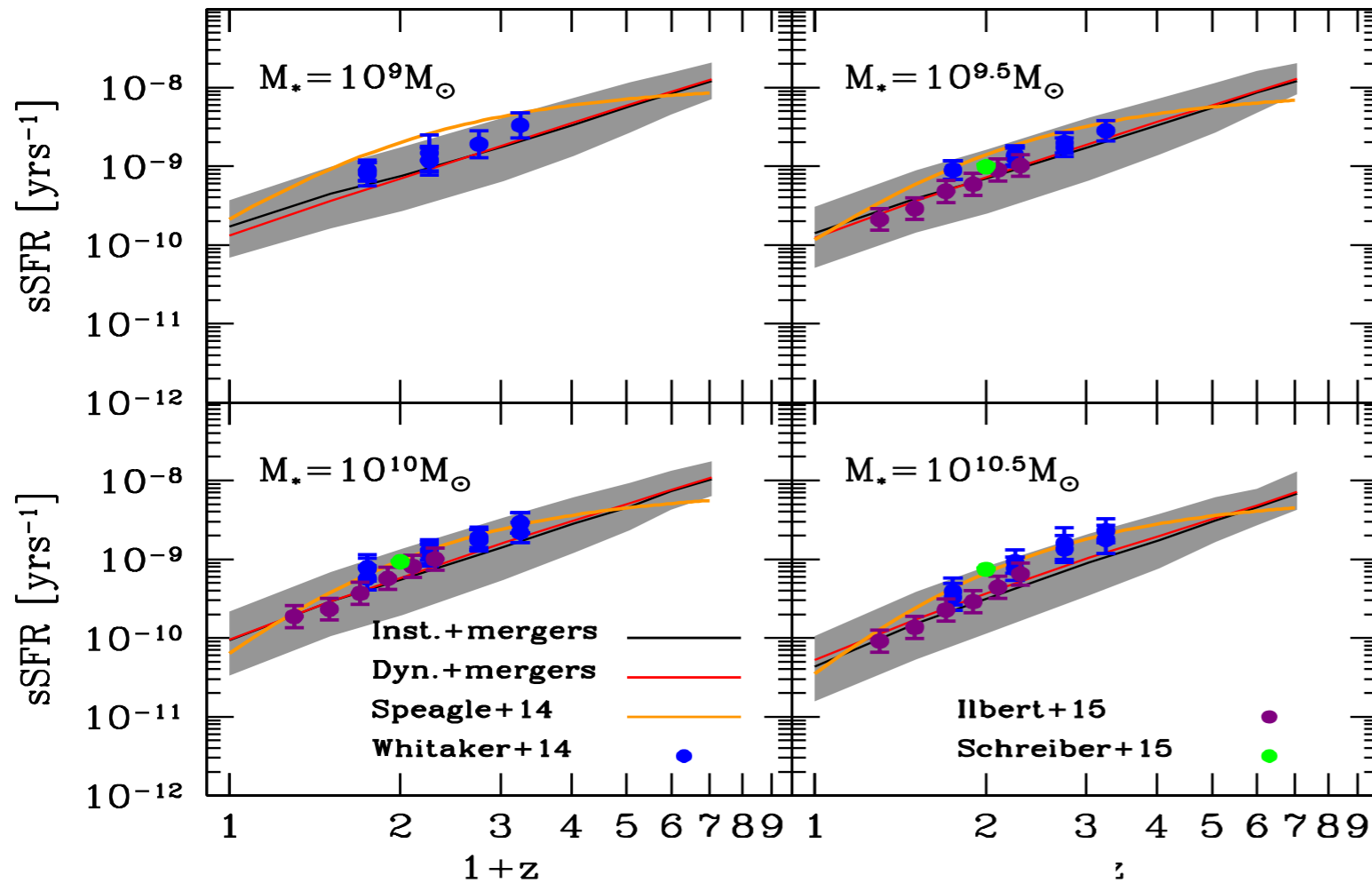
**Consistent with observations!**



# Is Main Sequence SFR Controlled by Halo Mass Accretion?

by Aldo Rodríguez-Puebla, Joel Primack, Peter Behroozi, Sandra Faber **MNRAS 2016**

**SHARC correctly predicts star formation rates to  $z \sim 4$**



**SHARC predicts “Age Matching” (blue galaxies in accreting halos) and “Galaxy Conformity” at low  $z$**

**Open Questions:**

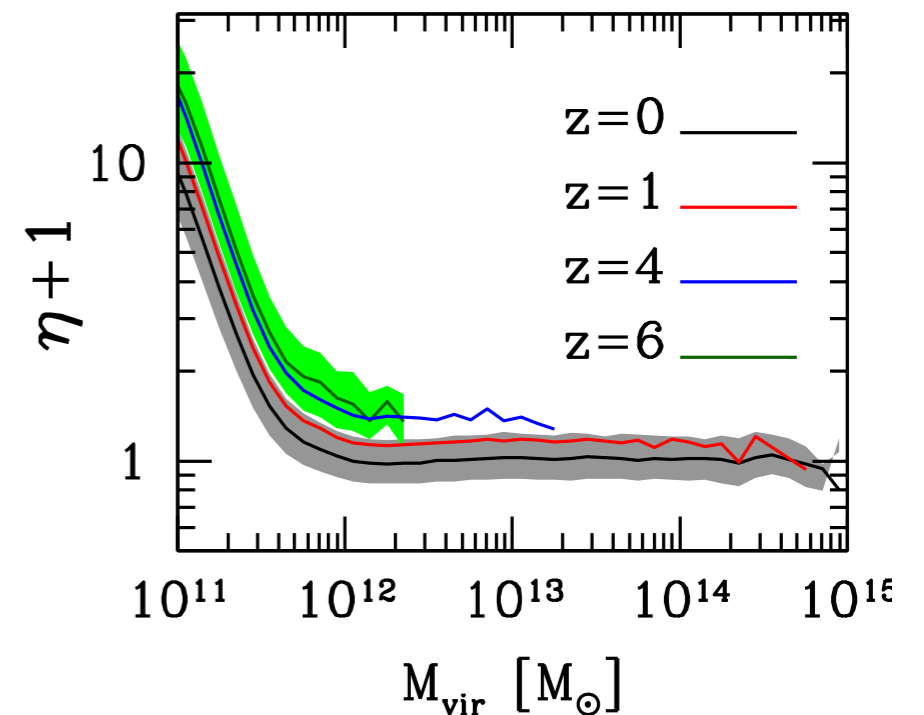
Extend SHARC to higher-mass galaxies

Also take quenching into account

Does SHARC correctly predict the growth rate of central galaxy stellar mass from the accretion rate of their halos? Test this in simulations!



We put **SHARC** in “bathtub” equilibrium models of galaxy formation & predict mass loading and metallicity evolution



Net mass loading factor  $\eta$  from an equilibrium bathtub model (E+SHARC)

# Constraining the Galaxy Halo Connection: Star Formation Histories, Galaxy Mergers, and Structural Properties

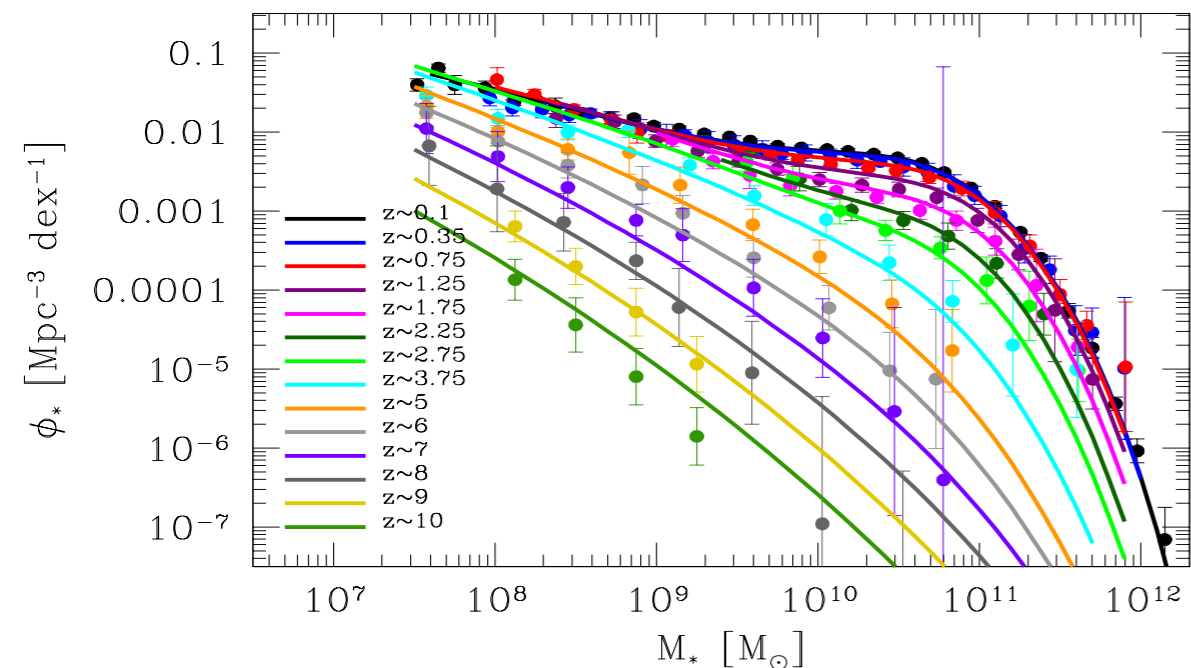
Aldo Rodriguez-Puebla, Joel Primack, Vladimir Avila-Reese, Sandra Faber [MNRAS in press](#)

Author	Redshift <sup>a</sup>	$\Omega$ [deg <sup>2</sup> ]	Corrections
Bell et al. (2003)	$z \sim 0.1$	462	I+SP+C
Yang, Mo & van den Bosch (2009a)	$z \sim 0.1$	4681	I+SP+C
Li & White (2009)	$z \sim 0.1$	6437	I+P+C
Bernardi et al. (2010)	$z \sim 0.1$	4681	I+SP+C
Bernardi et al. (2013)	$z \sim 0.1$	7748	I+SP+C
Rodriguez-Puebla et al. in prep	$z \sim 0.1$	7748	S
Drory et al. (2009)	$0 < z < 1$	1.73	SP+C
Moustakas et al. (2013)	$0 < z < 1$	9	SP+D+C
Pérez-González et al. (2008)	$0.2 < z < 2.5$	0.184	I+SP+D+C
Tomczak et al. (2014)	$0.2 < z < 3$	0.0878	C
Ilbert et al. (2013)	$0.2 < z < 4$	2	C
Muzzin et al. (2013)	$0.2 < z < 4$	1.62	I+C
Santini et al. (2012)	$0.6 < z < 4.5$	0.0319	I+C
Mortlock et al. (2011)	$1 < z < 3.5$	0.0125	I+C
Marchesini et al. (2009)	$1.3 < z < 4$	0.142	I+C
Stark et al. (2009)	$z \sim 6$	0.089	I
Lee et al. (2012)	$3 < z < 7$	0.089	I+SP+C
González et al. (2011)	$4 < z < 7$	0.0778	I+C
Duncan et al. (2014)	$4 < z < 7$	0.0778	C
Song et al. (2015)	$4 < z < 8$	0.0778	I
This paper, Appendix D	$4 < z < 10$	0.0778	-

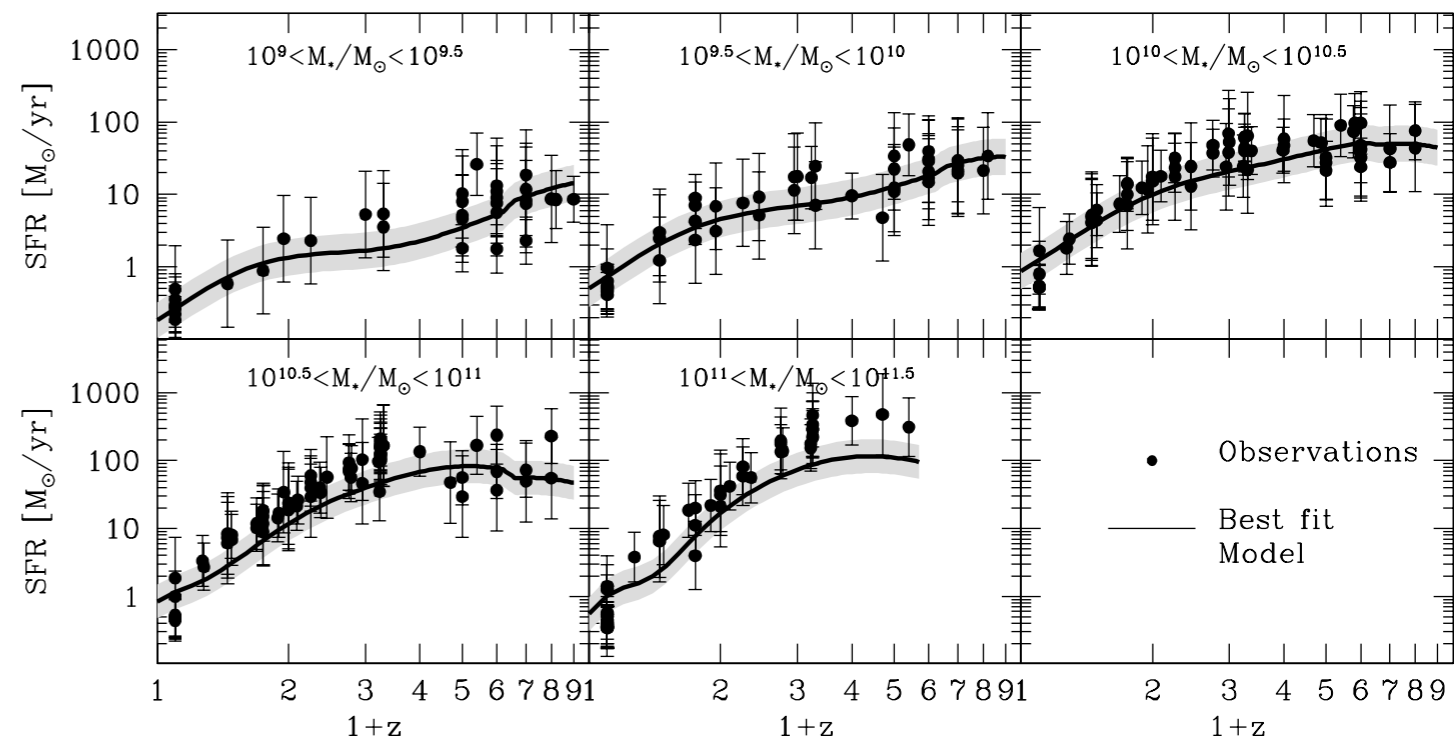
I=IMF; P= photometry corrections; S=Surface Brightness correction; D=Dust model;  
NE= Nebular Emissions; SP = SPS Model; C = Cosmology

Author	Redshift <sup>a</sup>	SFR Estimator	Corrections	Type
Chen et al. (2009)	$z \sim 0.1$	$H_\alpha/H_\beta$	S	All
Salim et al. (2007)	$z \sim 0.1$	UV SED	S	All
Noeske et al. (2007)	$0.2 < z < 1.1$	UV+IR	S	All
Karim et al. (2011)	$0.2 < z < 3$	1.4 GHz	I+S+E	All
Dunne et al. (2009)	$0.45 < z < 2$	1.4 GHz	I+S+E	All
Kajisawa et al. (2010)	$0.5 < z < 3.5$	UV+IR	I	All
Whitaker et al. (2014)	$0.5 < z < 3$	UV+IR	I+S	All
Sobral et al. (2014)	$z \sim 2.23$	$H_\alpha$	I+S+SP	SF
Reddy et al. (2012)	$2.3 < z < 3.7$	UV+IR	I+S+SP	SF
Magdis et al. (2010)	$z \sim 3$	FUV	I+S+SP	SF
Lee et al. (2011)	$3.3 < z < 4.3$	FUV	I+SP	SF
Lee et al. (2012)	$3.9 < z < 5$	FUV	I+SP	SF
González et al. (2012)	$4 < z < 6$	UV+IR	I+NE	SF
Salmon et al. (2015)	$4 < z < 6$	UV SED	I+NE+E	SF
Bouwens et al. (2011)	$4 < z < 7.2$	FUV	I+S	SF
Duncan et al. (2014)	$4 < z < 7$	UV SED	I+NE	SF
Shim et al. (2011)	$z \sim 4.4$	$H_\alpha$	I+S+SP	SF
Steinhardt et al. (2014)	$z \sim 5$	UV SED	I+S	SF
González et al. (2010)	$z = 7.2$	UV+IR	I+NE	SF
This paper, Appendix D	$4 < z < 8$	FUV	I+E+NE	SF

I=IMF; S=Star formation calibration; E=Extinction; NE= Nebular Emissions; SP=SPS Model



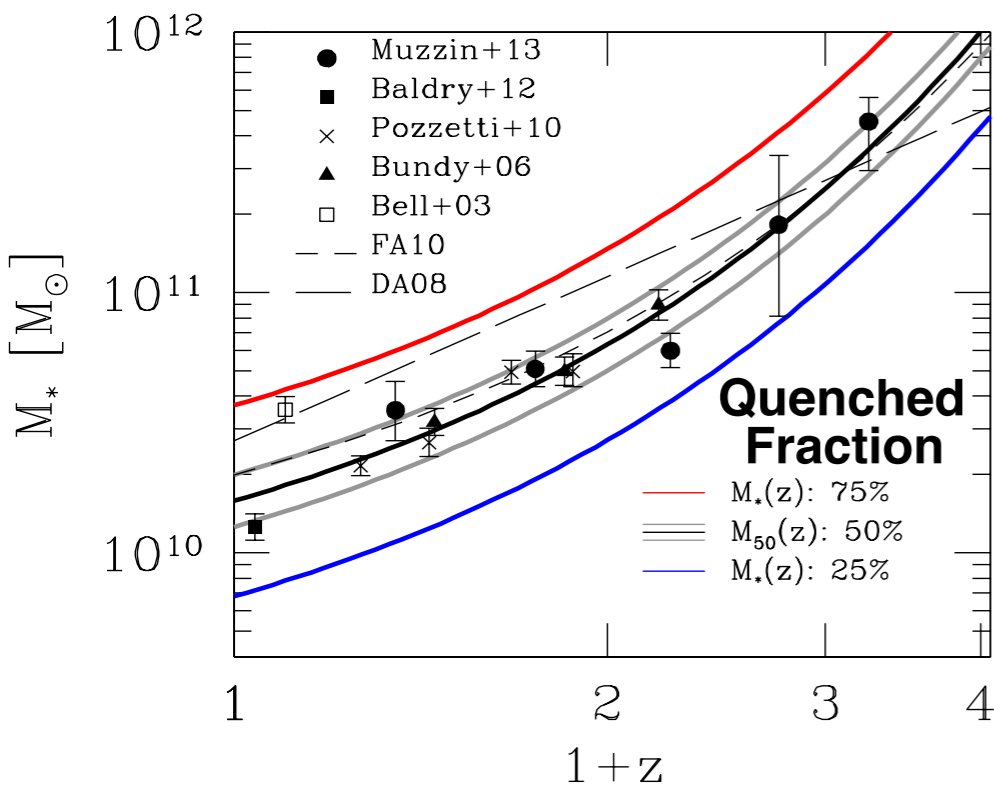
**Redshift evolution from  $z \sim 0.1$  to  $z \sim 10$  of the galaxy stellar mass function derived by using 20 observational samples from the literature and represented by filled circles with error bars. The various data has been corrected for potential systematics that could affect our results. Solid lines are the best fit model from a set of  $3 \times 10^5$  MCMC trials.**



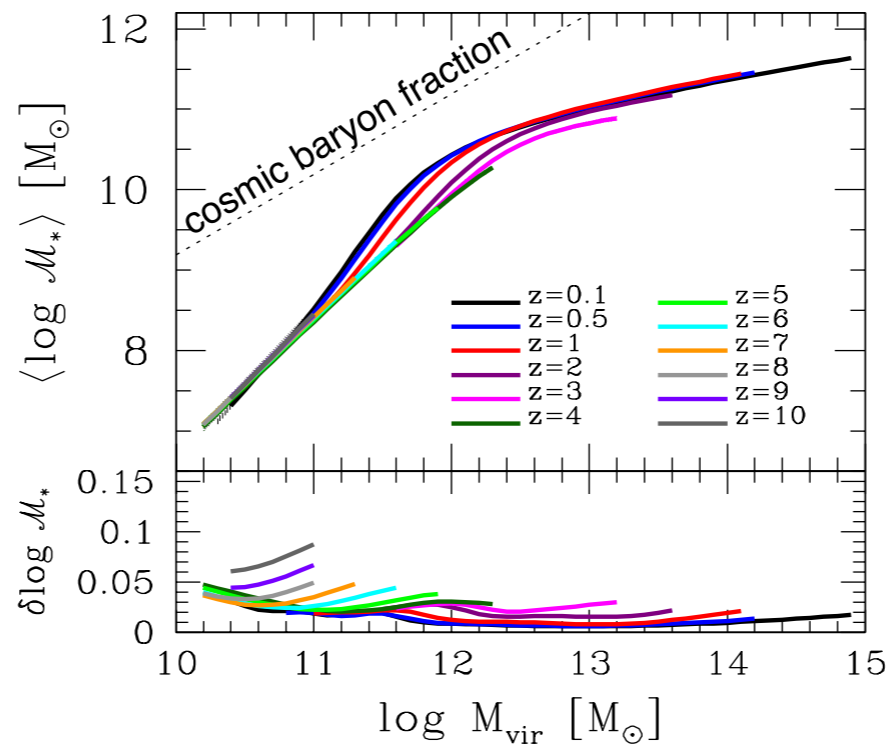
**Star formation rates as a function of redshift  $z$  in five stellar mass bins. Filled circles with error bars show the observed data. Black solid lines show our best fit model to the SFRs.**

# Constraining the Galaxy Halo Connection: Star Formation Histories, Galaxy Mergers, and Structural Properties

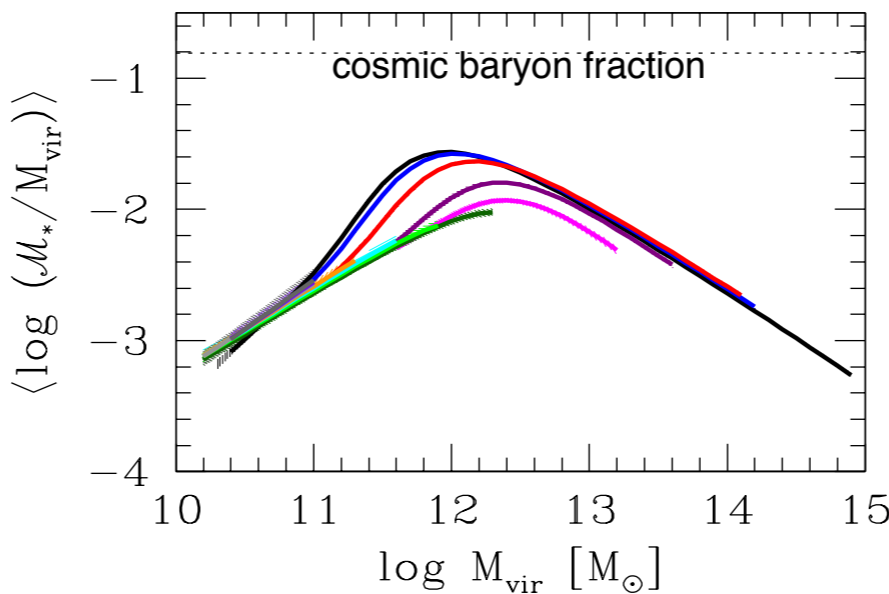
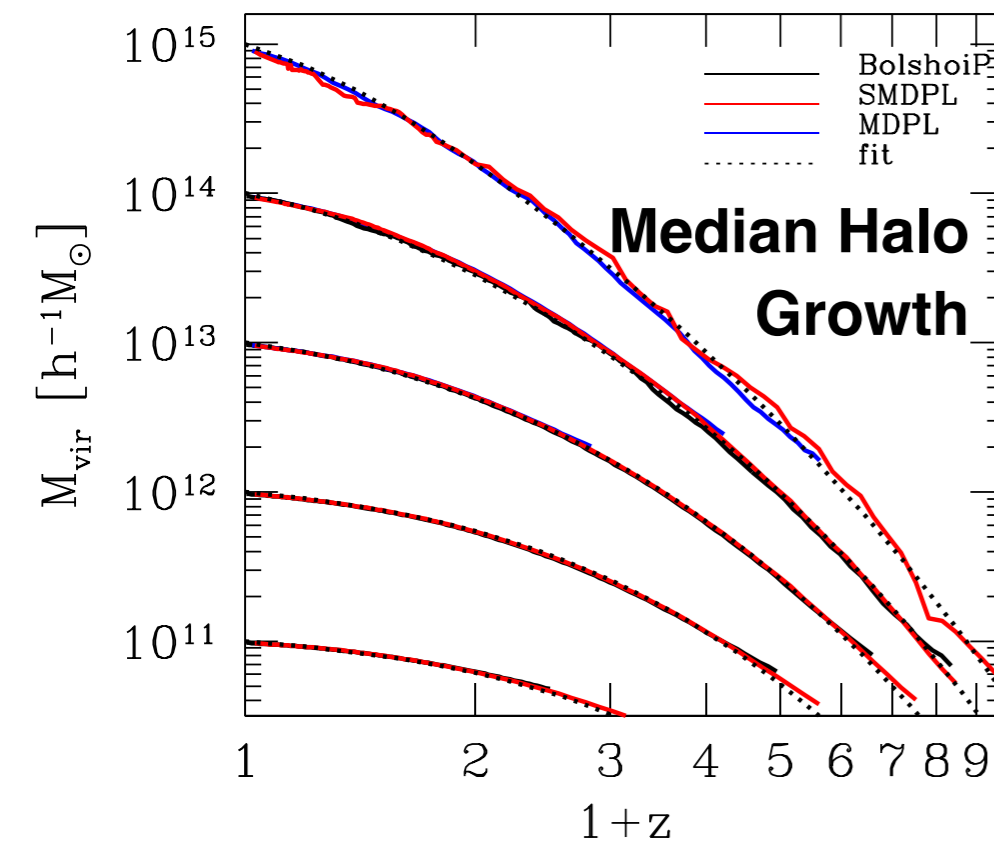
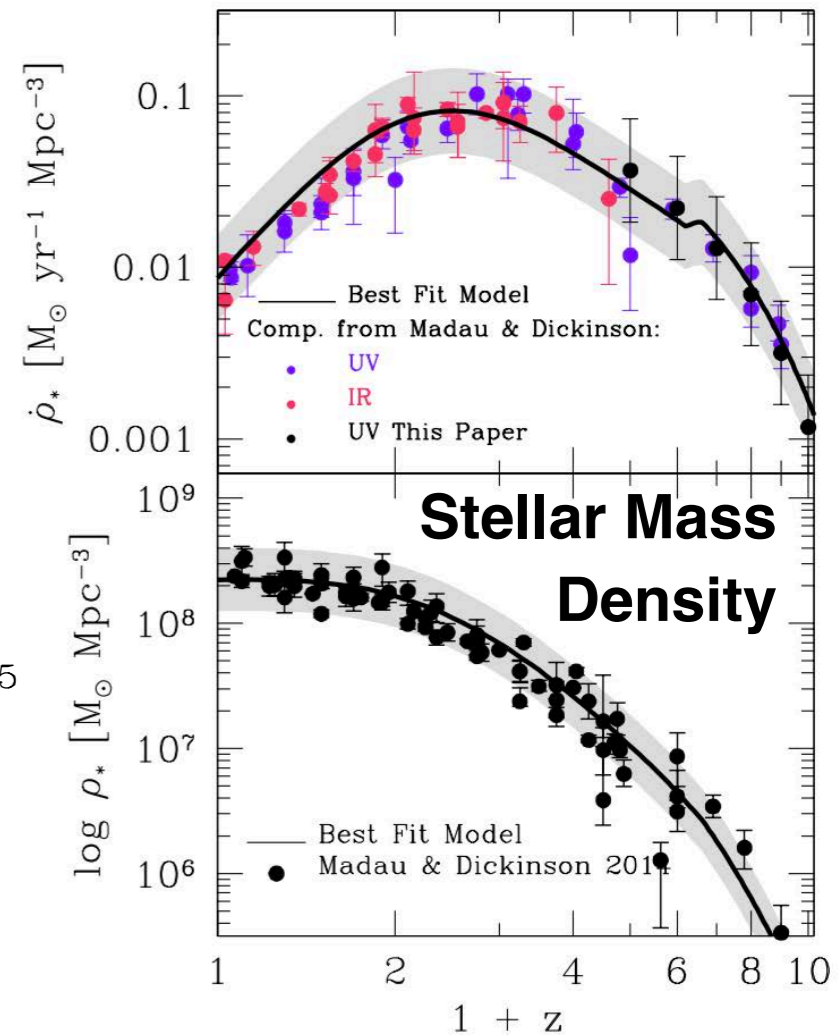
Aldo Rodriguez-Puebla, Joel Primack, Vladimir Avila-Reese, Sandra Faber [MNRAS in press](#)



## Average Stellar Mass Halo Mass Relation



## Star Formation Rate Density

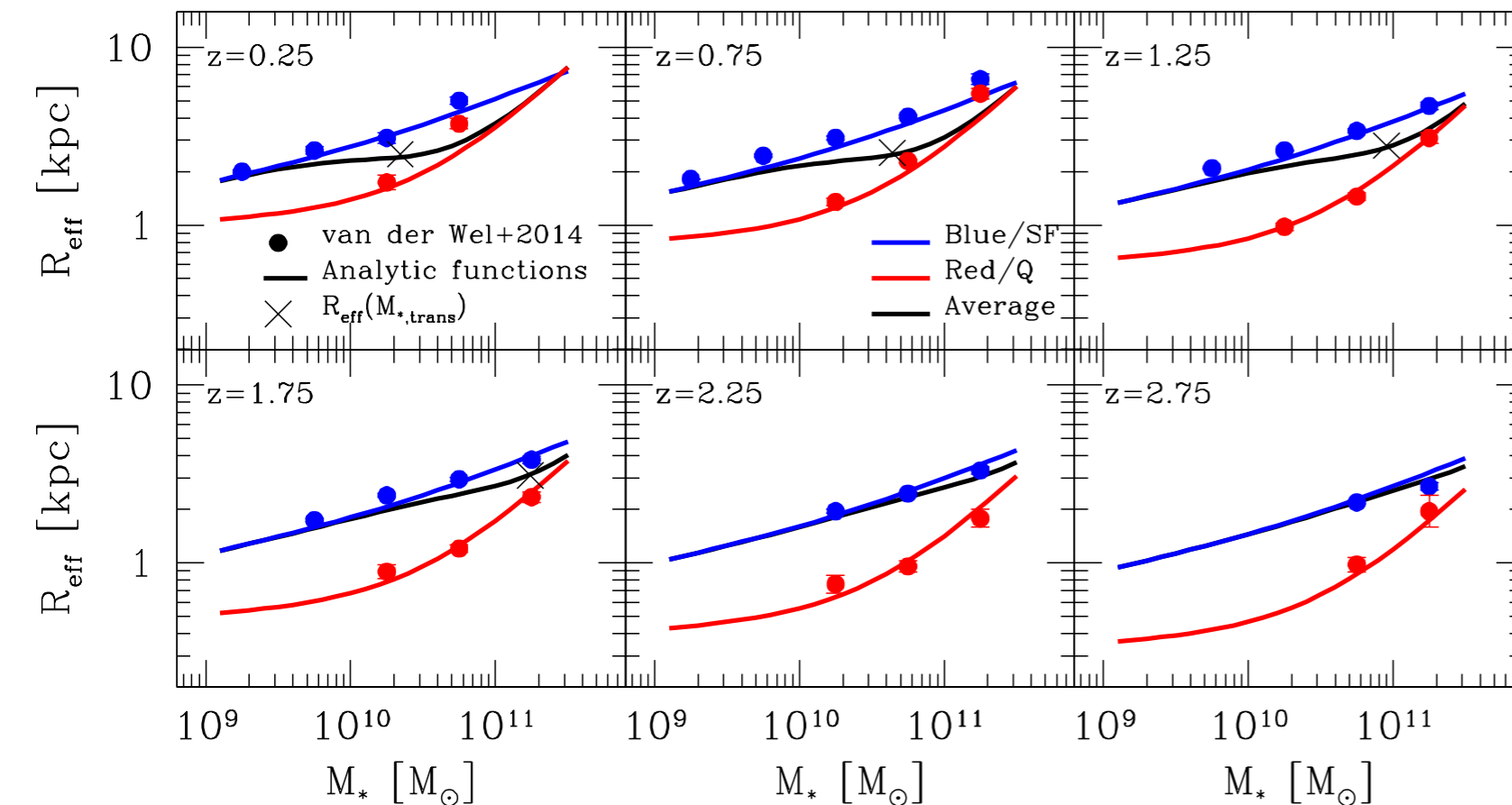
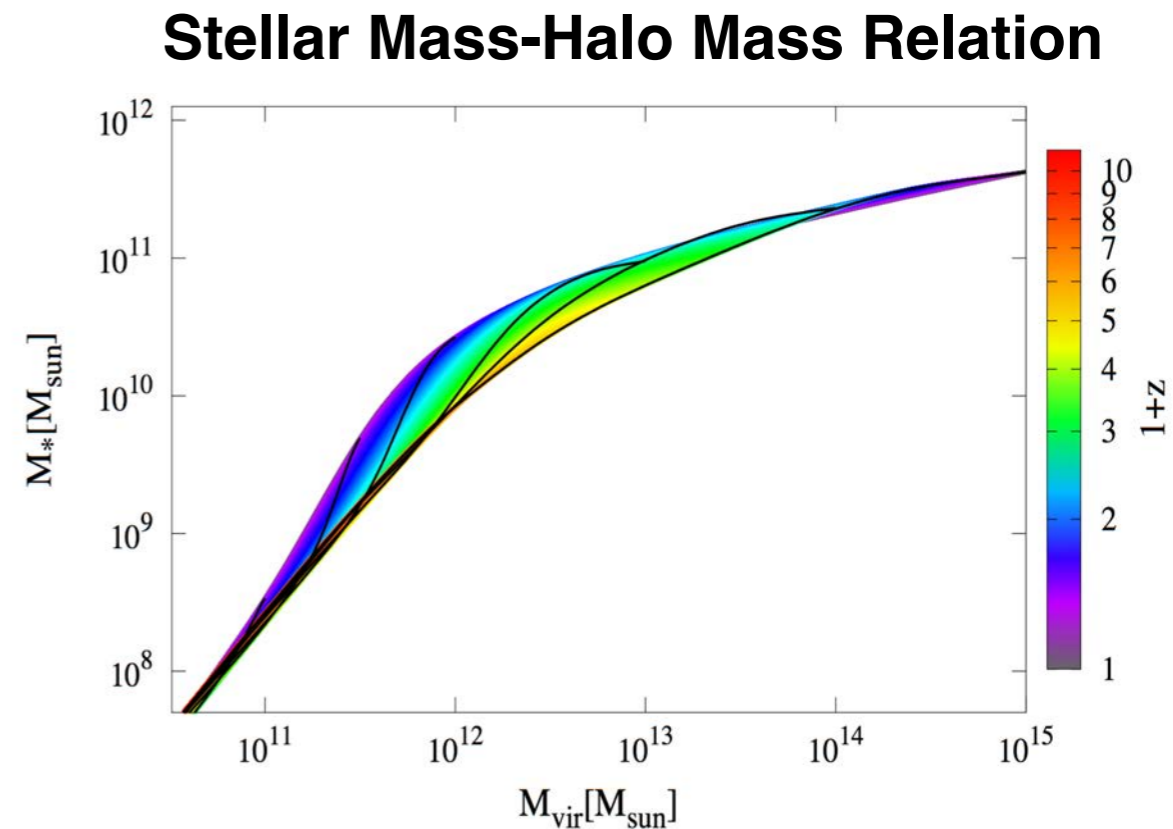
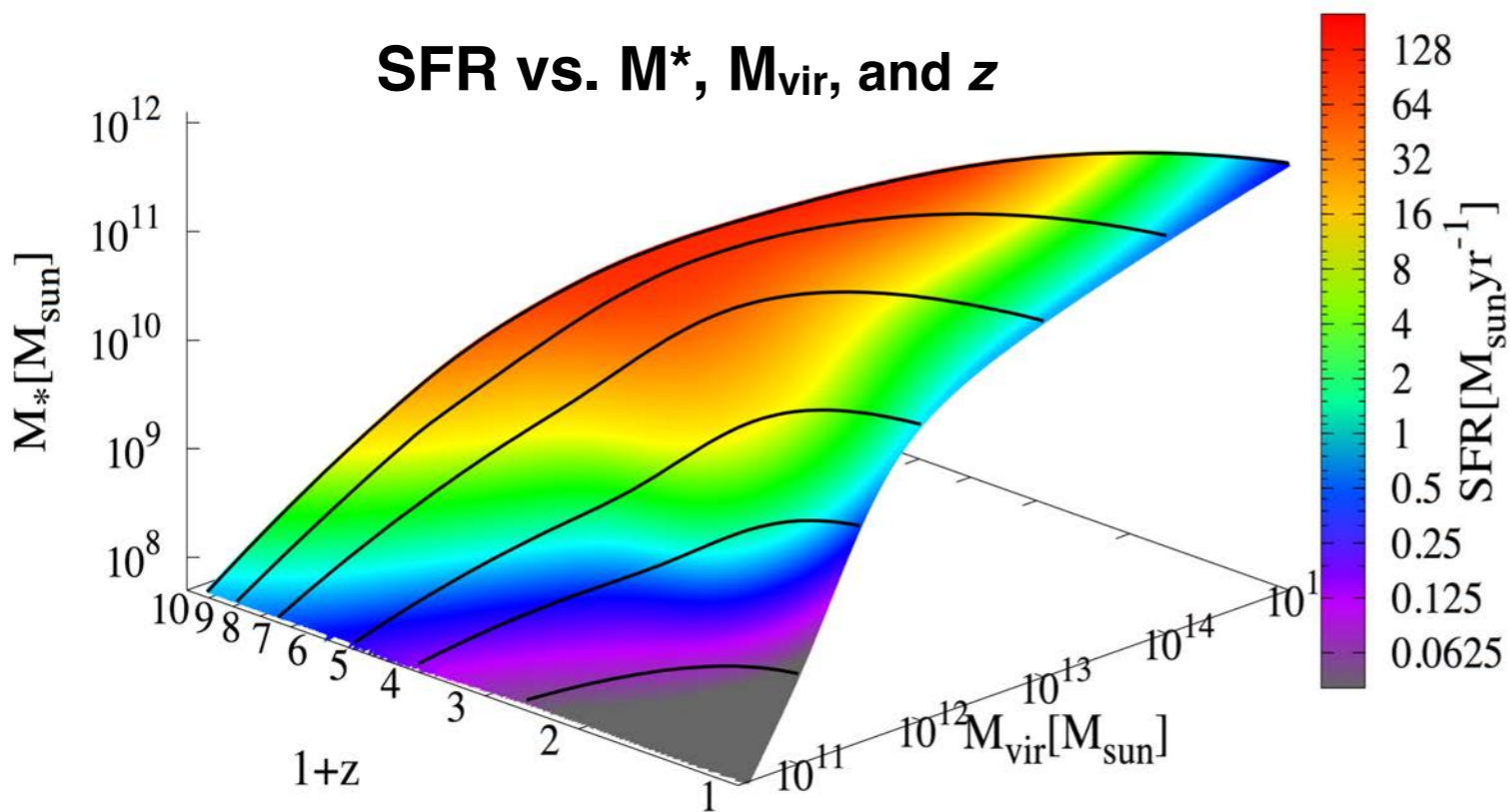




# Constraining the Galaxy Halo Connection:

## Star Formation Histories, Galaxy Mergers, and Structural Properties

Aldo Rodriguez-Puebla, Joel Primack, Vladimir Avila-Reese, Sandra Faber **MNRAS in press**



### Galaxy Radial Stellar Mass Distribution

Solid lines show the redshift dependence for blue and red galaxies of the local relation by Mosleh, Williams & Franx (2013) based on the MPA-JHU SDSS DR7. The black solid lines show the average circularized effective radius as a function of stellar mass. The crosses show the effective radius at  $M_{50}$ , the stellar mass at which the quenched fraction of galaxies is 50%. We utilize the plotted redshift dependences as an input to derive the average galaxy's radial mass distribution as a function of stellar mass by **assuming that blue/star-forming galaxies have a Sersic index  $n = 1$  while red/quenched galaxies have a Sersic index  $n = 4$ .**

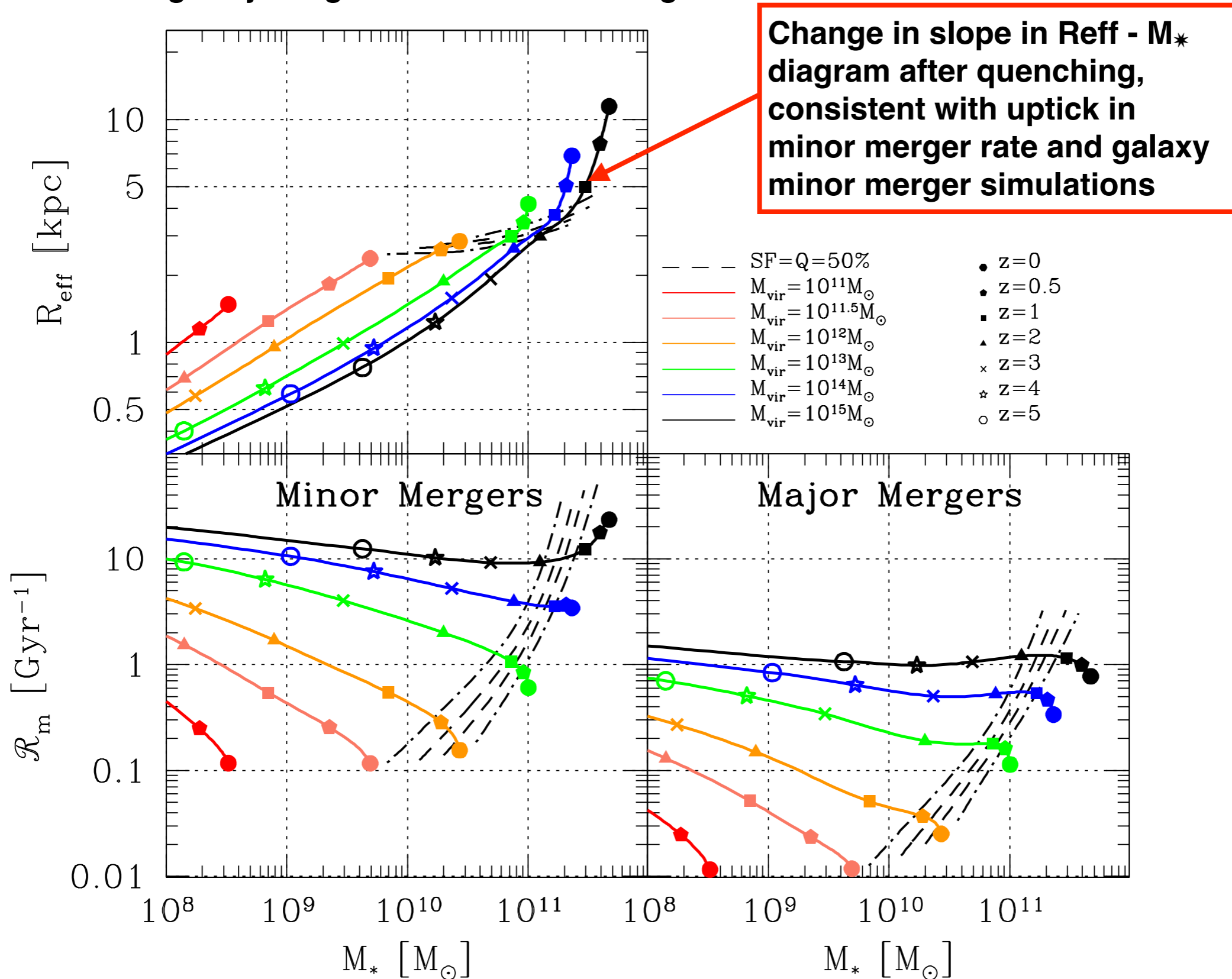


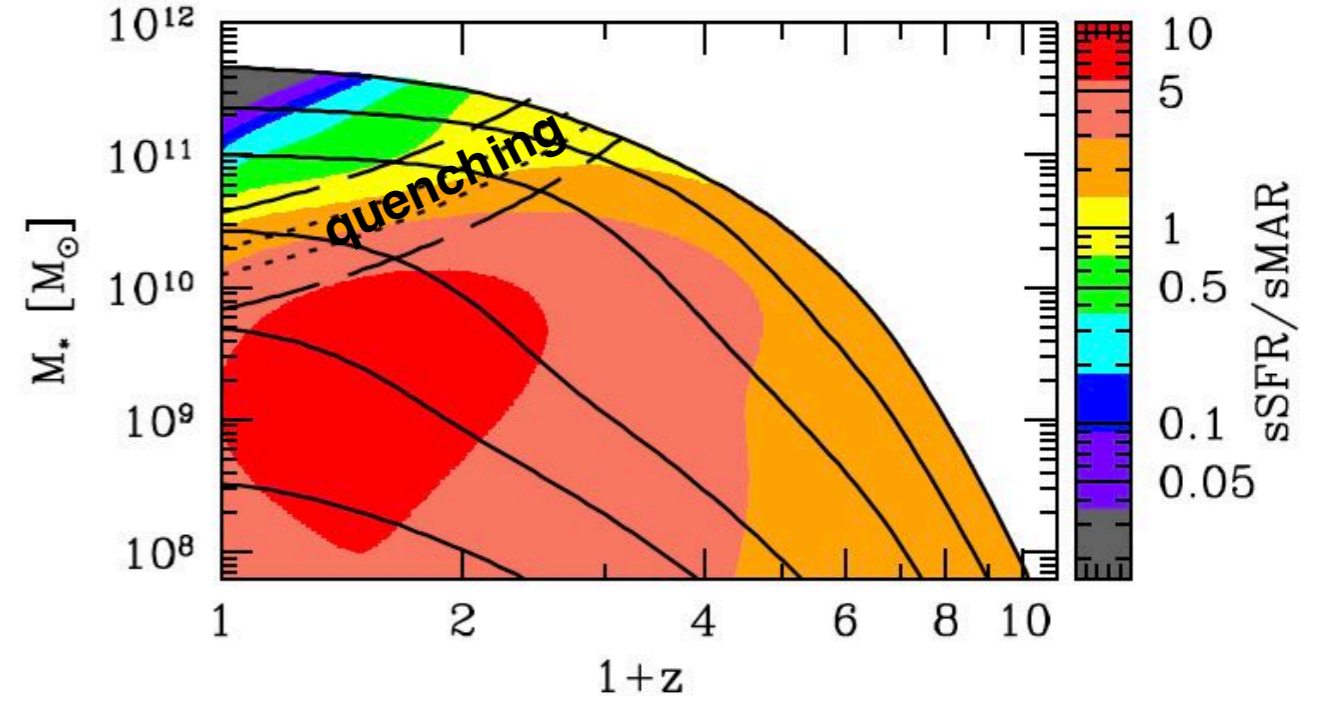
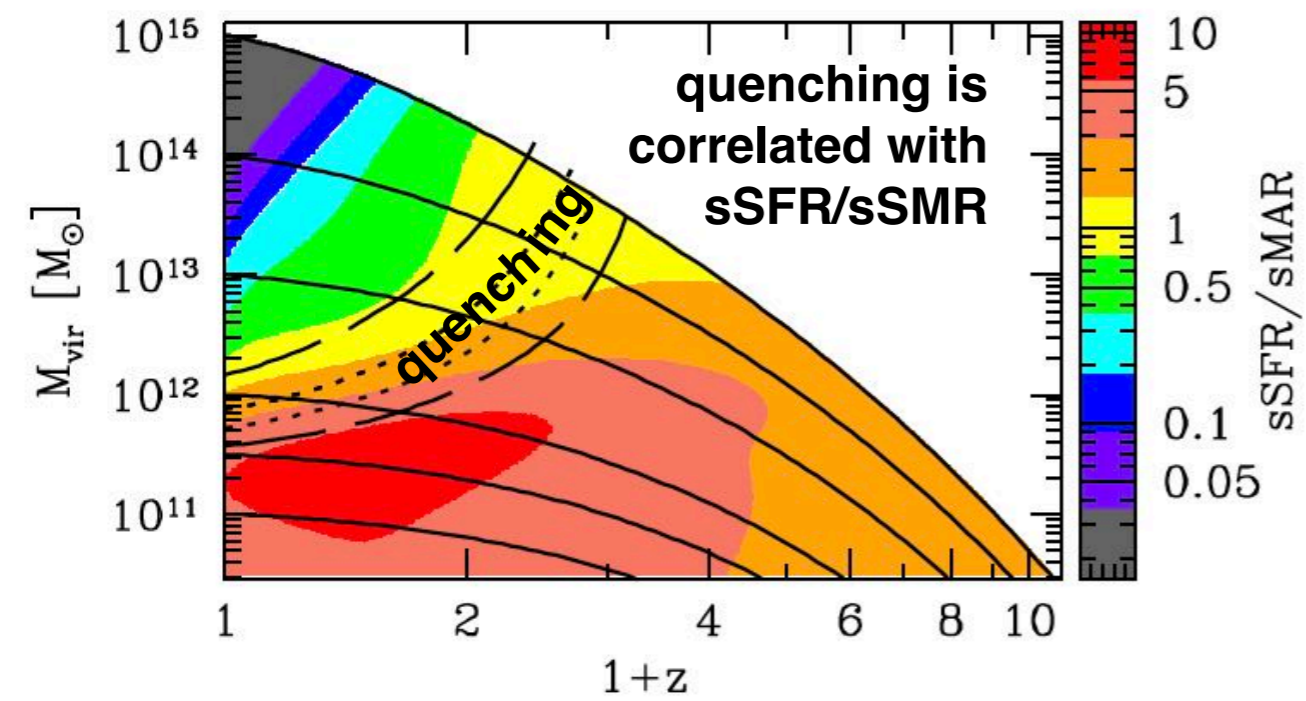
# Constraining the Galaxy Halo Connection:

## Star Formation Histories, Galaxy Mergers, and Structural Properties

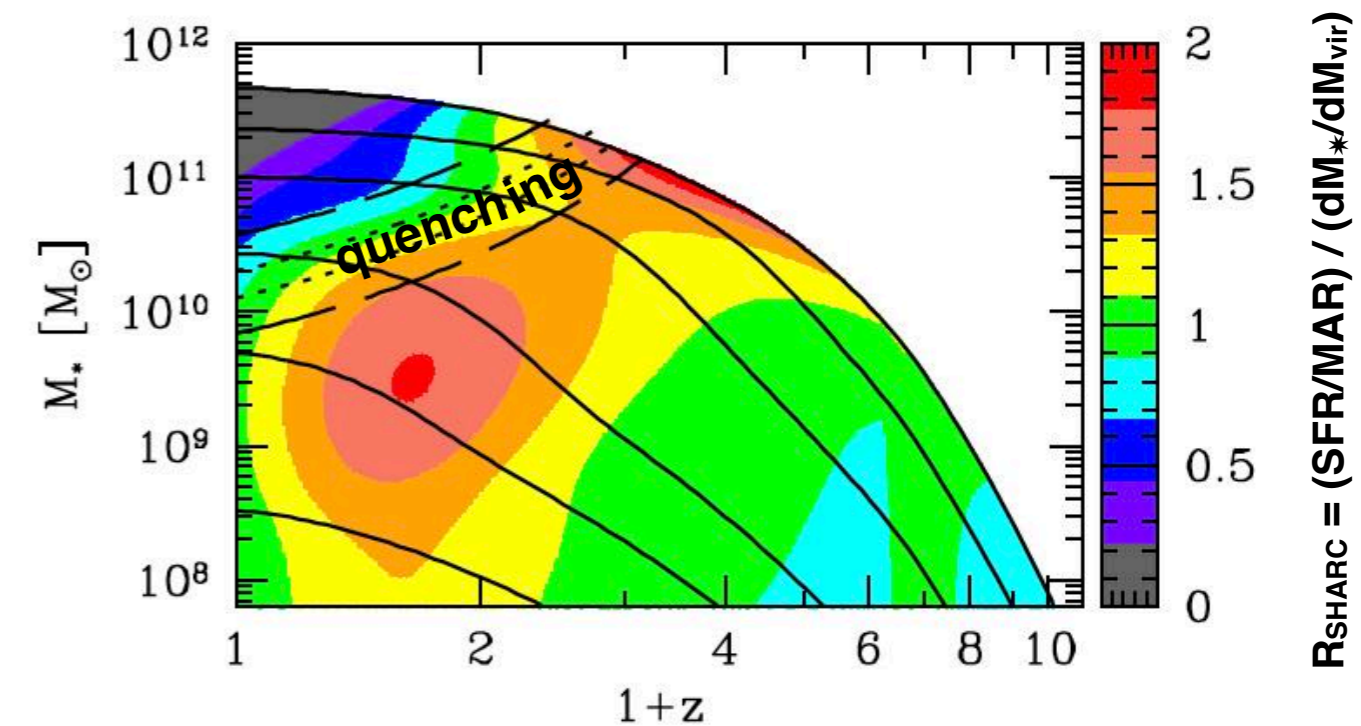
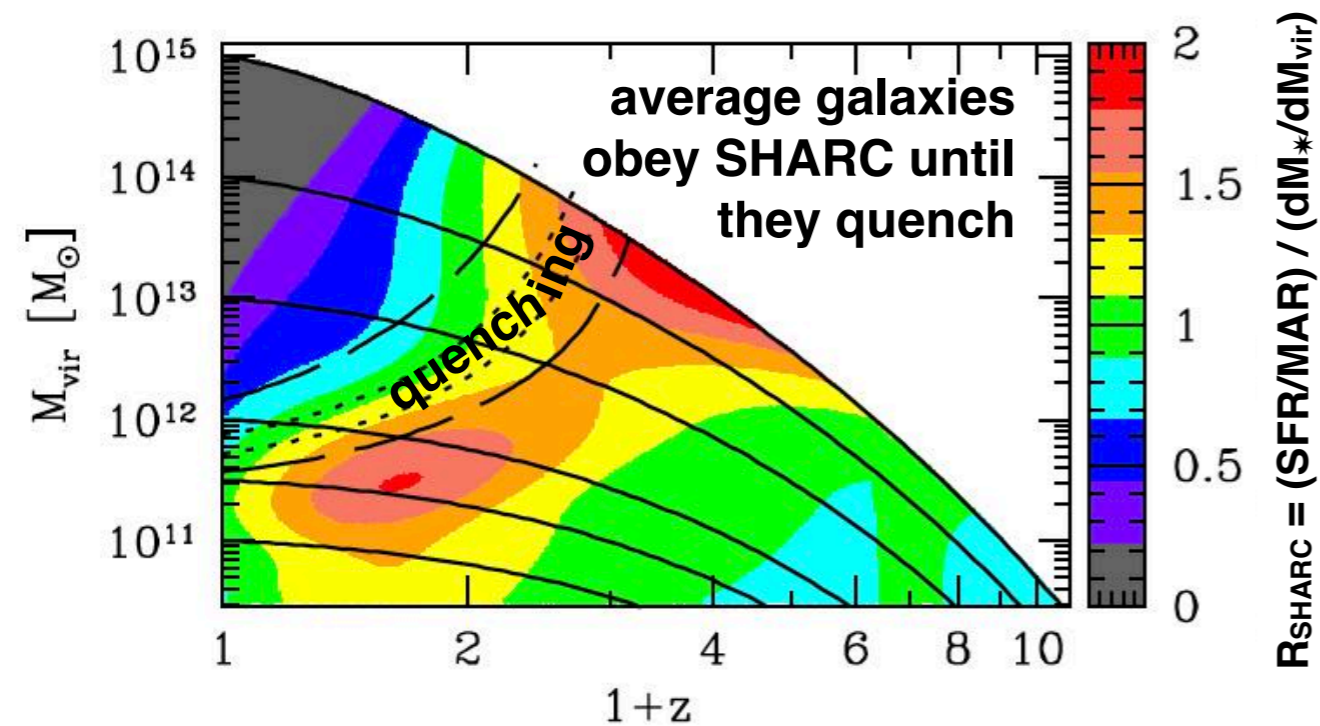
Aldo Rodriguez-Puebla, Joel Primack, Vladimir Avila-Reese, Sandra Faber [MNRAS in press](#)

We infer galaxy merger rates from halo mergers





This figure shows that quenching is correlated with  $sSFR/sSMR = t_{\text{halo}}/t_*$ , since  $sSFR/sSMR$  and quenching curves are nearly parallel.  $sSFR/sSMR$  - first rises, reaching a peak  $\sim 2$  at  $z \sim 3$  for  $10^{13}$  halos, a peak  $\sim 7$  for  $10^{12}$  halos at  $z \sim 1.5$ , and  $10^{11}$  halos are still at peak  $sSFR/sSMR \sim 10$  - then declines along all  $M_{\text{vir}}$  and  $M_*$  progenitor tracks toward  $z=0$ .



This figure shows that the SHARC approximation is rather well satisfied until quenching, the SHARC ratio  $R_{\text{SHARC}} = (\text{SFR} / \text{MAR}) / (dM_{\text{vir}}/d\log M_*)$  having a value of about 1 to 2 along the progenitor trajectories, and then dropping after quenching. This shows quenching is correlated with  $R_{\text{SHARC}}$  :

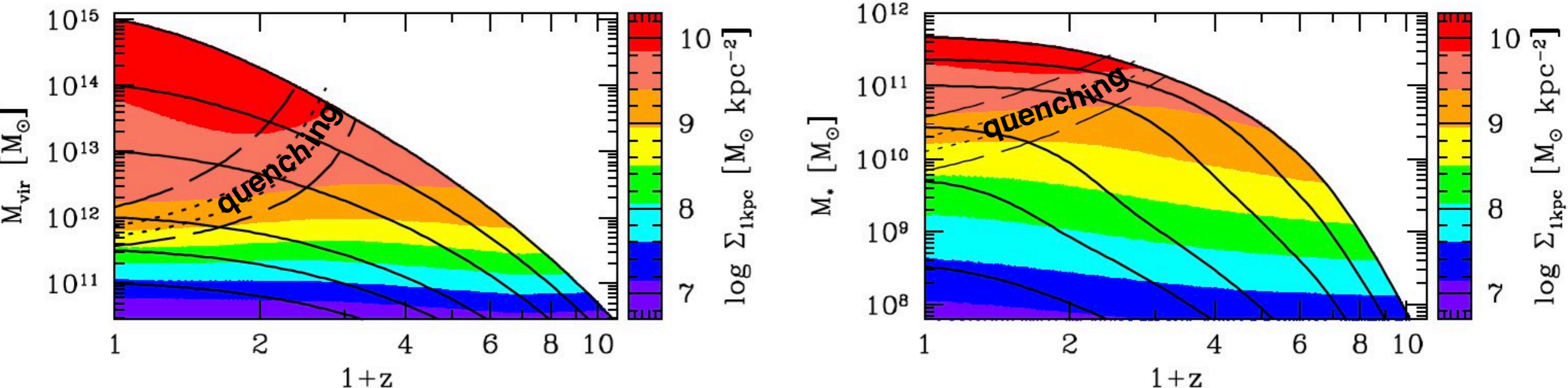
- the fraction of quenched galaxies is  $\sim 50\%$  when  $R_{\text{SHARC}} \sim 1$  to 1.5, and the quenched fraction is  $> 75\%$  when  $R_{\text{SHARC}}$  drops to  $\sim 1$
- like  $sSFR/sSMR$ ,  $R_{\text{SHARC}}$  first rises along all progenitor curves, reaches a peak at higher  $z$  for higher mass ( $M_{\text{vir}}$  or  $M_*$ ), and then declines
- unlike  $sSFR/sSMR$ , the peak SHARC ratio is nearly constant between 1.5 and 2 (the SHARC ratio peaks at about 2 for both  $10^{11.5}$  halos at  $z \sim 0.5$  and  $10^{15}$  halos at  $z \sim 3$ , and at about 1.5 for intermediate mass halos).

Note: the SHARC formula is  $\text{SFR} = (dM_*/dM_{\text{vir}}) \text{MAR}$  where  $\text{MAR} = dM_{\text{vir}}/dt$ . Define  $R_{\text{SHARC}} = (\text{SFR} / \text{MAR}) / (dM_*/dM_{\text{vir}})$ , so SHARC  $\implies R_{\text{SHARC}} = 1$ .



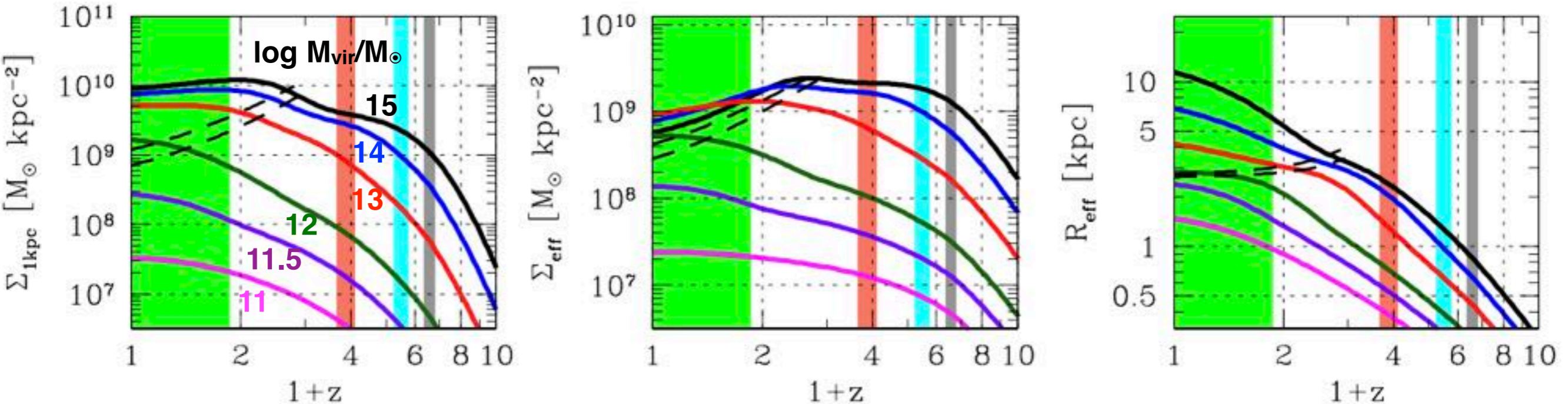
# Constraining the Galaxy Halo Connection: Star Formation Histories, Galaxy Mergers, and Structural Properties

Aldo Rodriguez-Puebla, Joel Primack, Vladimir Avila-Reese, Sandra Faber MNRAS in press



This figure (and the left panel below) shows that  $\Sigma_1$  reaching a maximum correlates with quenching:

- $\Sigma_1$  at the quenching transition rises steadily with  $M_{vir}$  and reaches maximum at lower  $z$  for lower  $M_{vir}$  – “quenching downsizing”
- That the progenitor tracks are parallel to the trajectory curves shows that  $\Sigma_1$  remains constant after it reaches its maximum



The right panel shows that  $R_{eff}$  steadily rises along halo trajectories, and quenching typically occurs when  $R_{eff} \approx 3$  kpc. Although  $\Sigma_1$  is flat after quenching, the middle panel shows that  $\Sigma_{eff}$  declines after quenching as  $R_{eff}$  increases.



[https://132.248.1.39/galaxy/galaxy\\_halo.html](https://132.248.1.39/galaxy/galaxy_halo.html)

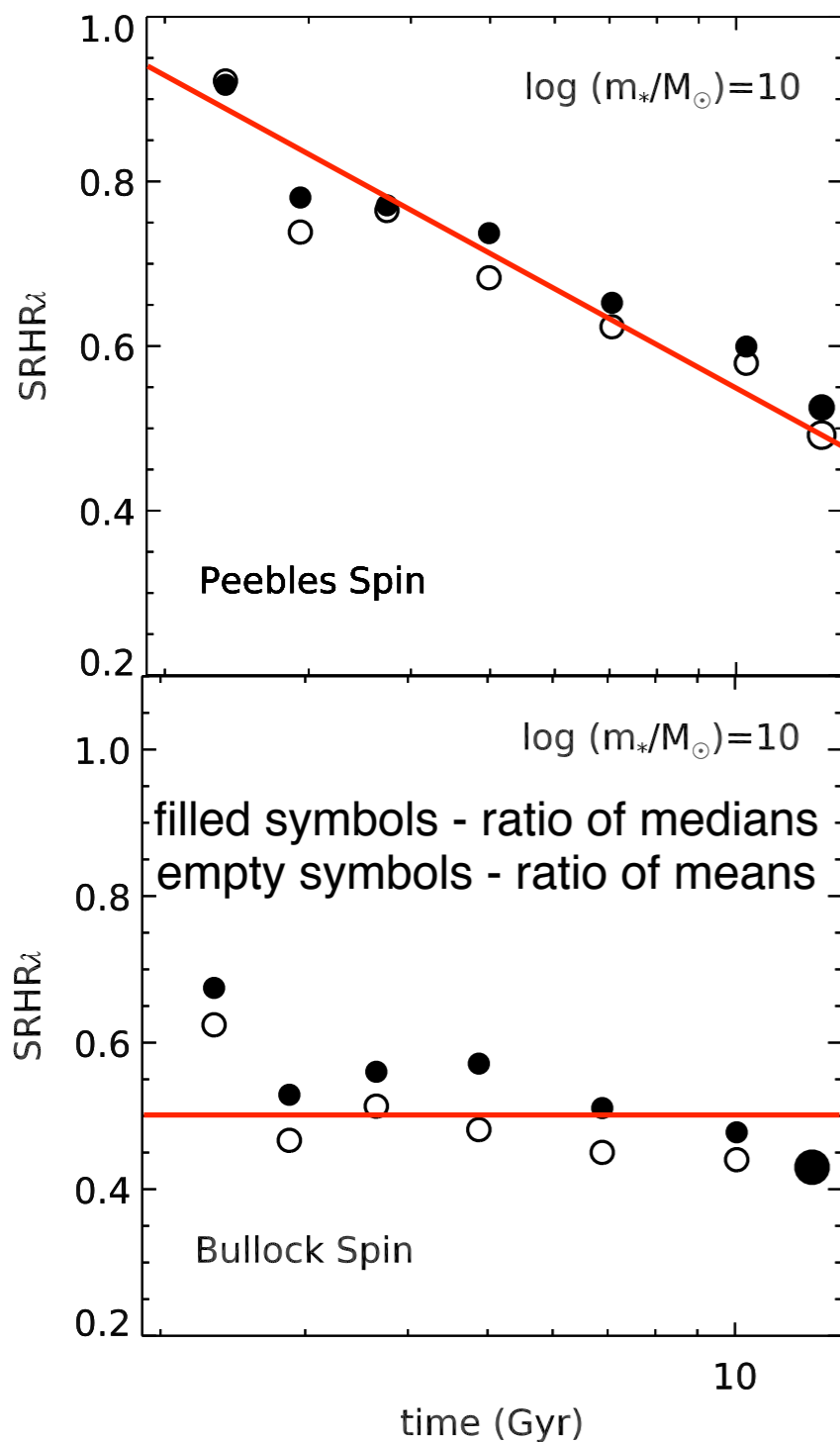
THE  
GALAXY-HALO CONNECTION  
PROJECT

HOW CAN I HELP YOU?



# The Relationship between Galaxy and Dark Matter Halo Size from $z \sim 3$ to the Present

Rachel Somerville et al. 2017



$$\text{SRHR}_\lambda \equiv R_{3D}^*/(\lambda R_{\text{halo}})$$

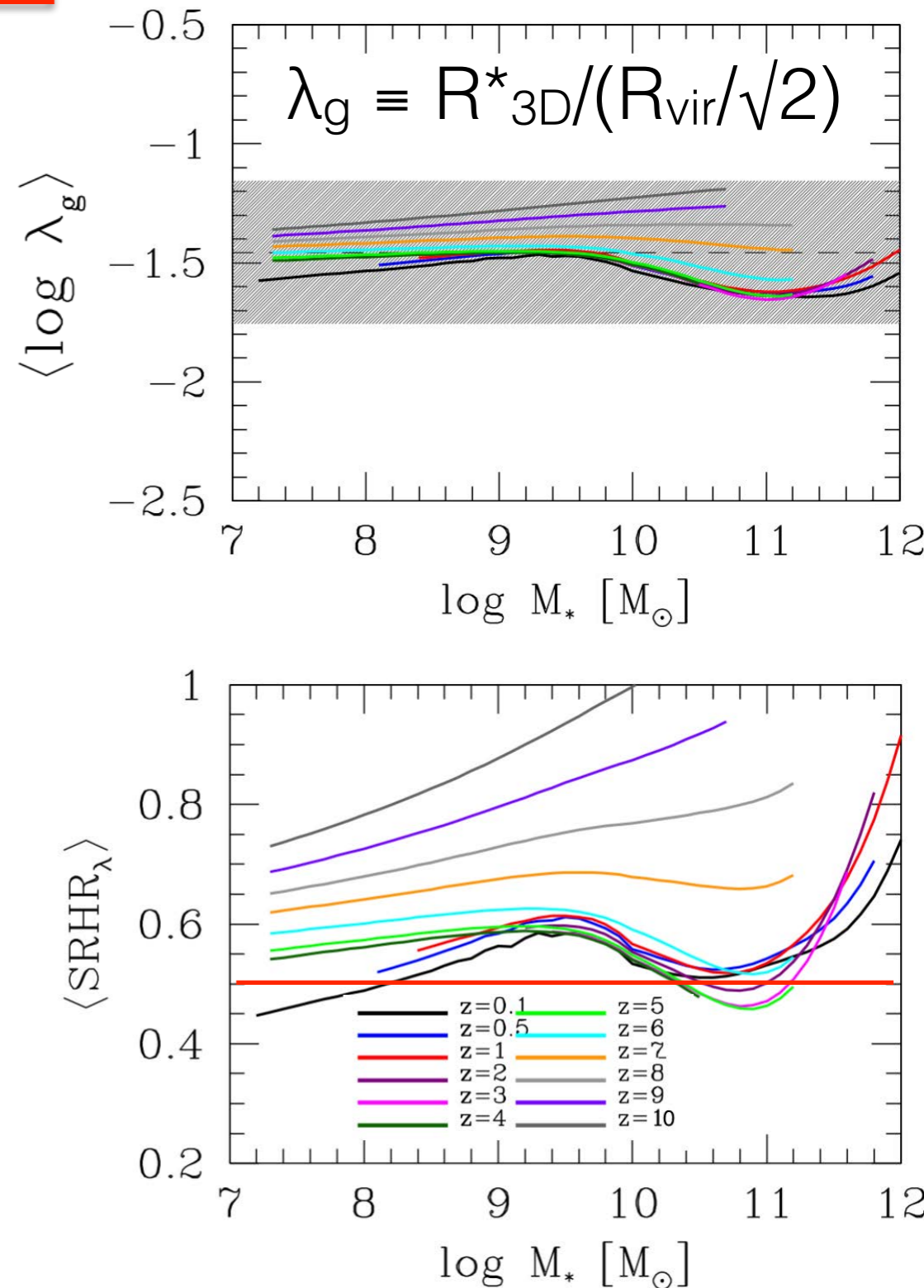
$$\lambda_P = \frac{J|E|^{1/2}}{GM_{\text{vir}}^{5/2}}$$

$\lambda_P(z)$  decreases with increasing  $z$  partly because of decreasing  $|E|$

$$\lambda_B = \frac{J}{\sqrt{2}M_{\text{vir}}V_{\text{vir}}R_{\text{vir}}}$$

**$R_{3D}^* \approx 0.5 \lambda_B R_{\text{halo}}$  at all redshifts  $0 < z < 3$  for  $M^* = 10^{10} M_\odot$ , where  $\lambda_B = \langle \lambda_B \rangle \approx 0.035$**

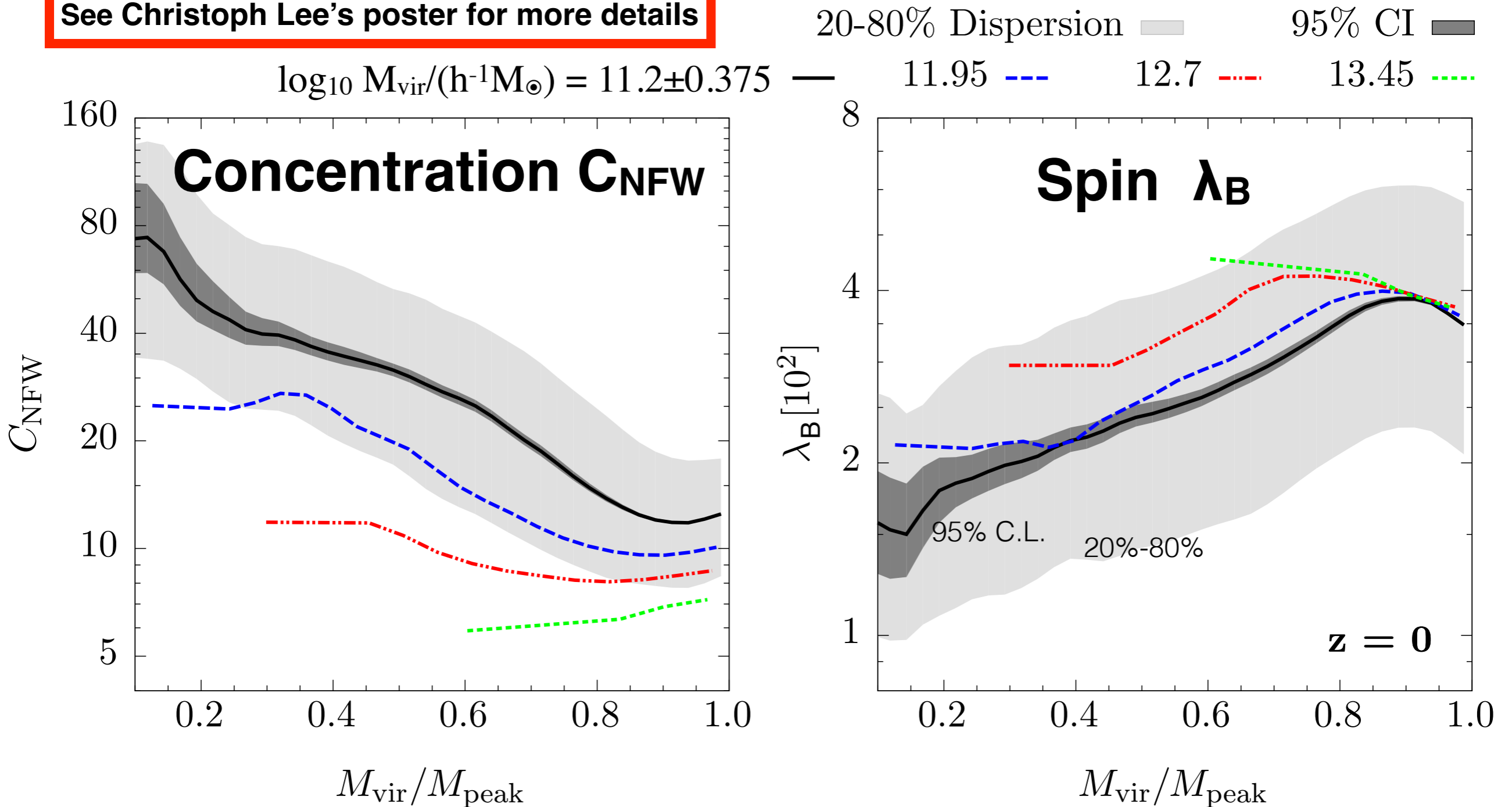
# Behavior of typical galaxies, using methods of Rodriguez-Puebla, Primack, et al. 2017 abundance matching paper



# Causes & Consequences of Halo Mass Loss

Christoph T. Lee, Joel R. Primack, Peter Behroozi, Aldo Rodríguez-Puebla, Doug Hellinger, Austin Tuan, Jessica Zhu, Avishai Dekel  
to be submitted to MNRAS

See Christoph Lee's poster for more details



- Most low mass halos in dense regions are significantly stripped
- Halos that have lost 5-15% of their mass relative to  $M_{\text{peak}}$  have lower  $C_{\text{NFW}}$ , higher  $\lambda_{\text{B}}$
- Halos that have lost more than  $\sim 20\%$  of their mass have higher  $C_{\text{NFW}}$  and lower  $\lambda_{\text{B}}$

# Properties of Dark Matter Haloes: Local Environment Density

Christoph T. Lee, Joel R. Primack, Peter Behroozi, Aldo Rodríguez-Puebla, Doug Hellinger, Avishai Dekel [MNRAS 2017](#)

## Low Mass

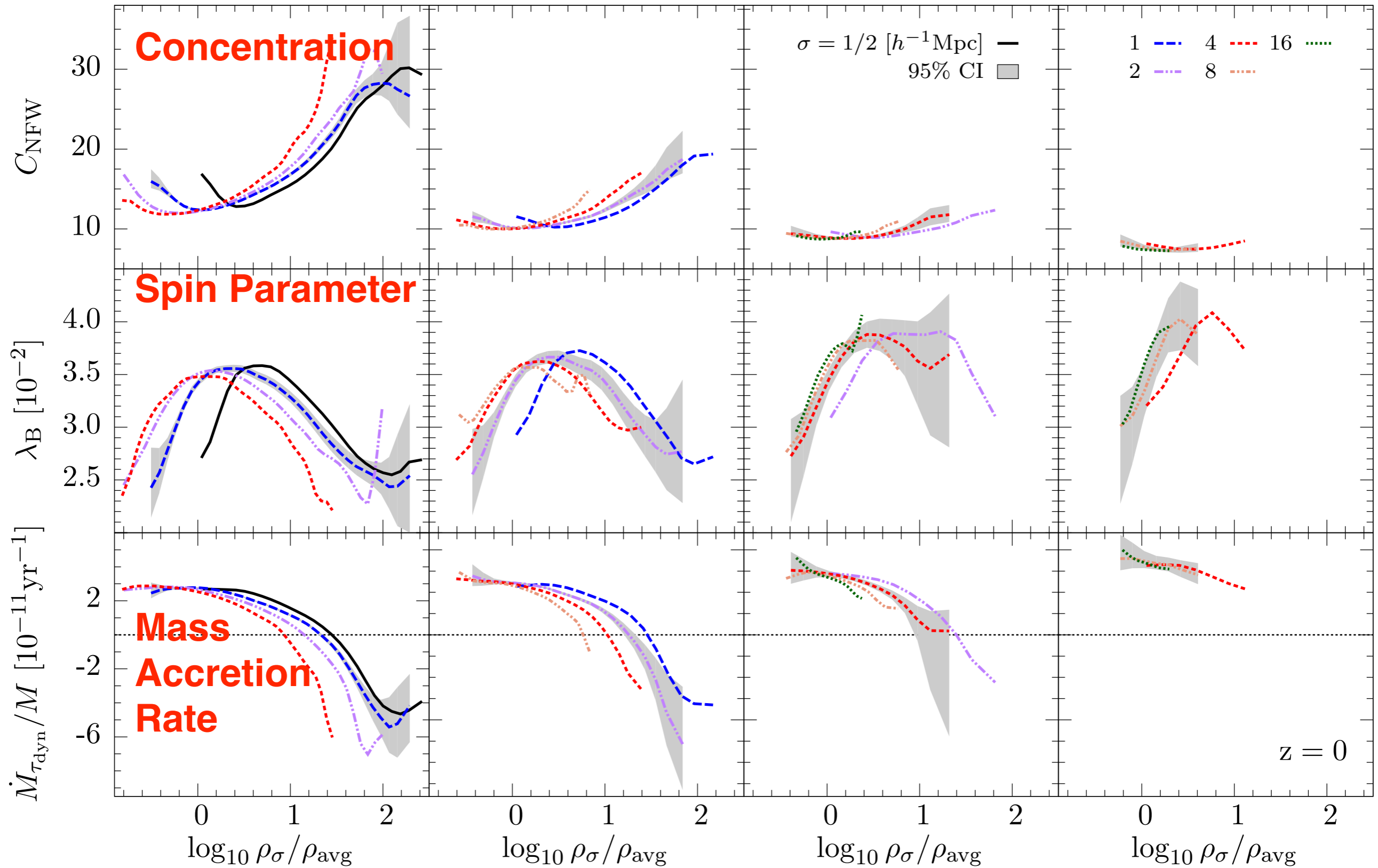
$\log_{10} M_{\text{vir}} / (h^{-1} M_{\odot}) = 11.200 \pm 0.375$

## Intermediate Mass

$11.95 \pm 0.375$

## High Mass

$13.45 \pm 0.375$



# Is Galaxy Radius $R_{3D}^* \propto \lambda R_{halo}$ ? Measure $R_{3D}^*$ vs. Local Density

Huertas-Company+13 found no difference vs. density, and Cebrian & Trujillo MNRAS 2017 find that galaxies in low-density regions are slightly larger.

## The effect of the environment on the stellar mass–size relationship for present-day galaxies

Maria Cebrian and Ignacio Trujillo [MNRAS 2014](#)

For every galaxy in our sample, we explore the surrounding density within 2 Mpc using two distinct estimators of the environment. We find that galaxies are slightly larger in the field than in high-density regions. This effect is more pronounced for late-type morphologies ( $\sim 7.5$  per cent larger) and especially at low masses ( $M_* < 2 \times 10^{10} M_\odot$ ), although it is also measurable in early-type galaxies ( $\sim 3.5$  per cent larger).

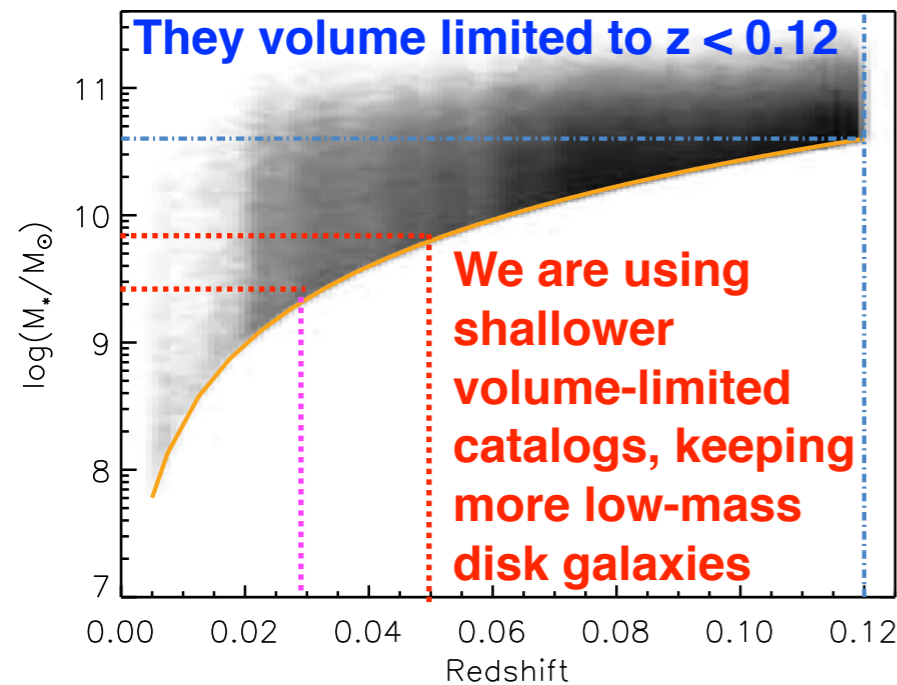
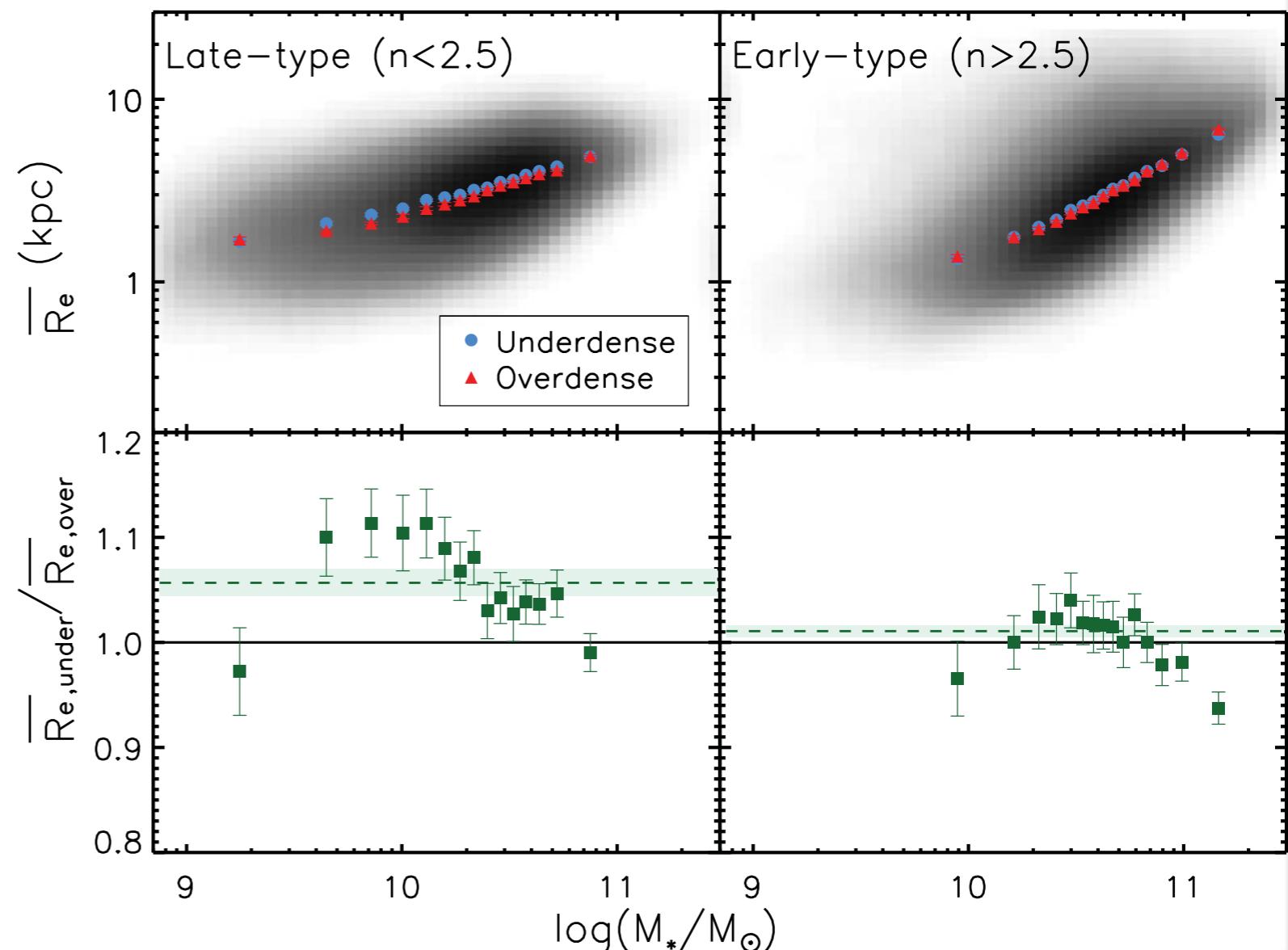


**Figure 4.** The redshift–mass plane of the stellar mass-complete galaxies in the NYU-VAGC. The solid orange line shows the mass-completeness line of the sample. The vertical and horizontal blue lines indicate the redshift and the mass limit used to explore the density of various environments. In order to lighten the plot, the density of objects is represented as a shaded surface instead of using individual points.

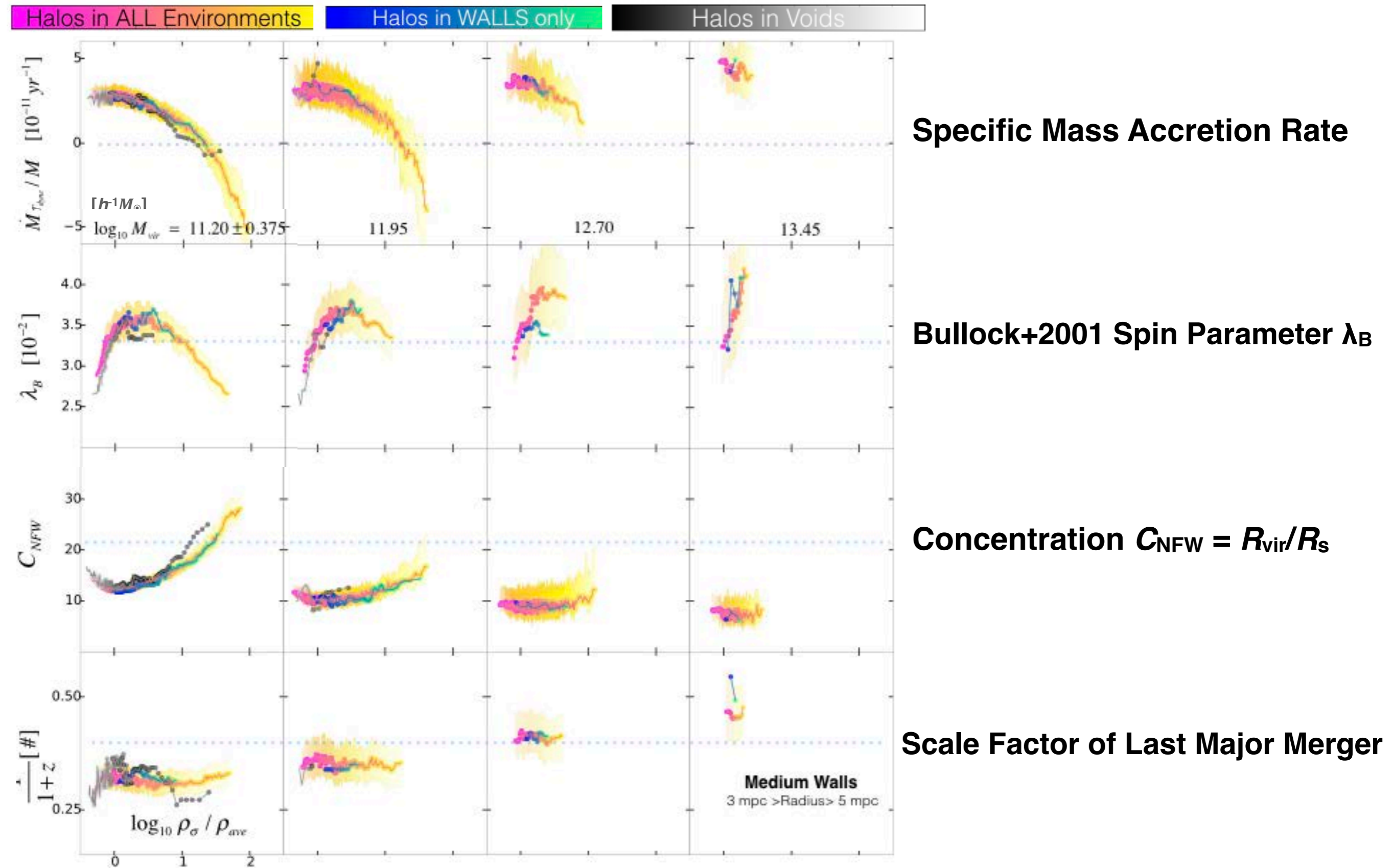


We are measuring  $R_{3D}^*$  vs. density in SDSS, and spin  $\lambda$  by the exact same methods in mock catalogs from Bolshoi-Planck and MultiDark-Planck.



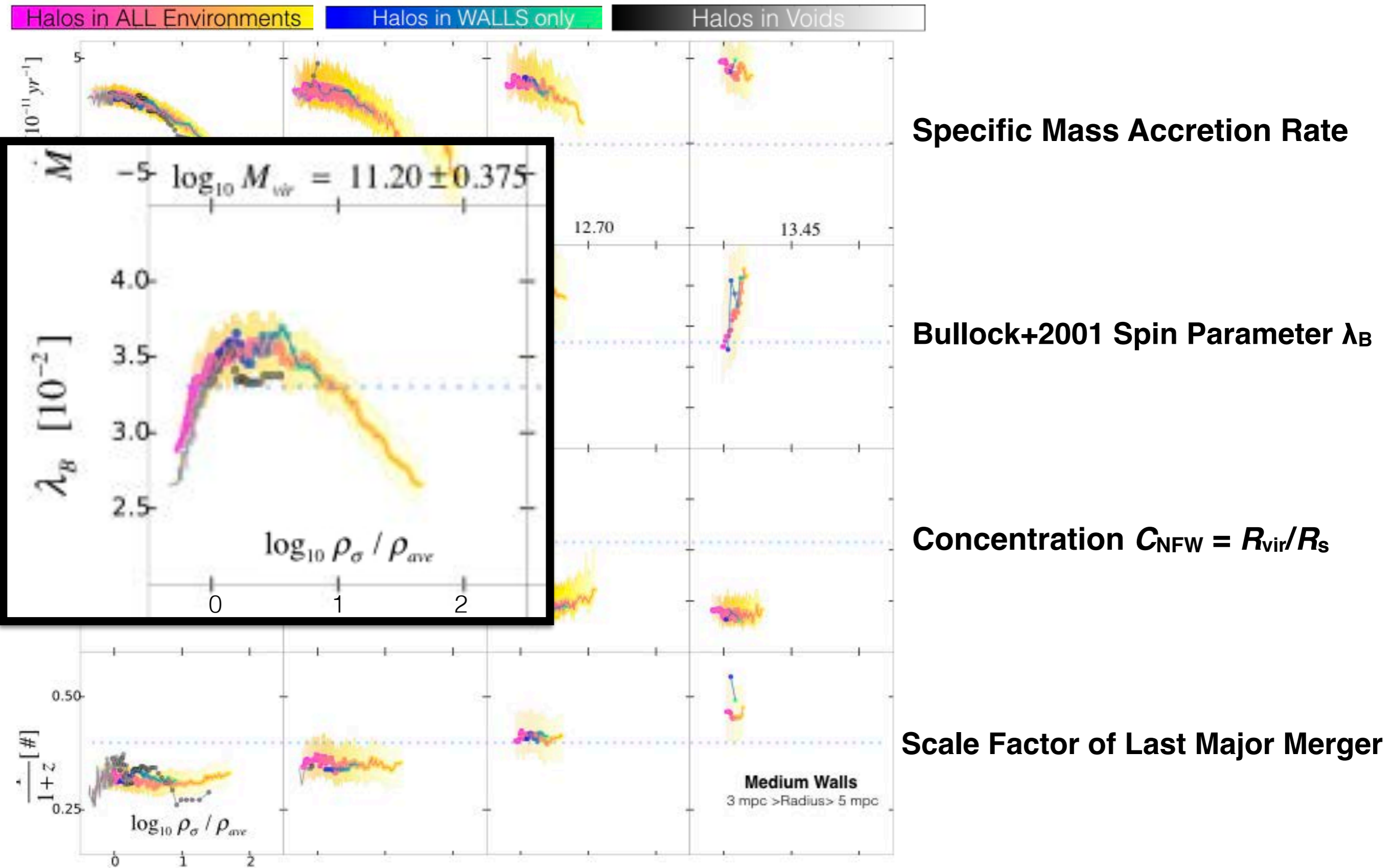
# Halo Properties Independent of Web Location at the Same Density

Tze Ping Goh, Christoph T. Lee, Joel R. Primack, Miguel Aragon Calvo, Peter Behroozi, Aldo Rodríguez-Puebla, Doug Hellinger, Avishai Dekel, Kathryn Johnston (in preparation)



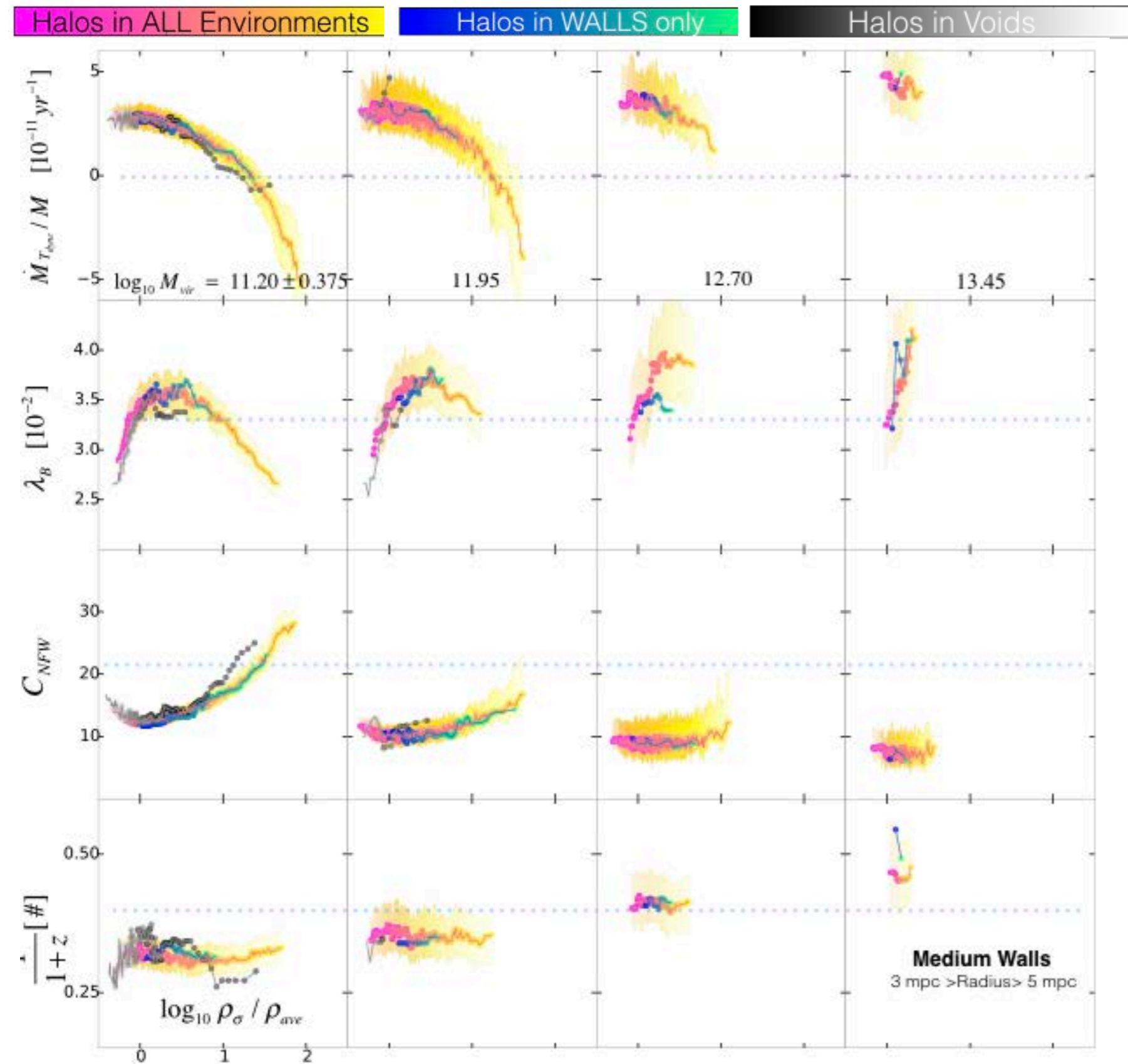
# Halo Properties Independent of Web Location at the Same Density

Tze Ping Goh, Christoph T. Lee, Joel R. Primack, Miguel Aragon Calvo, Peter Behroozi, Aldo Rodríguez-Puebla, Doug Hellinger, Avishai Dekel, Kathryn Johnston (in preparation)



# Halo Properties Independent of Web Location at the Same Density

Tze Ping Goh, Christoph T. Lee, Joel R. Primack, Miguel Aragon Calvo, Peter Behroozi, Aldo Rodríguez-Puebla, Doug Hellinger, Avishai Dekel, Kathryn Johnston (in preparation)



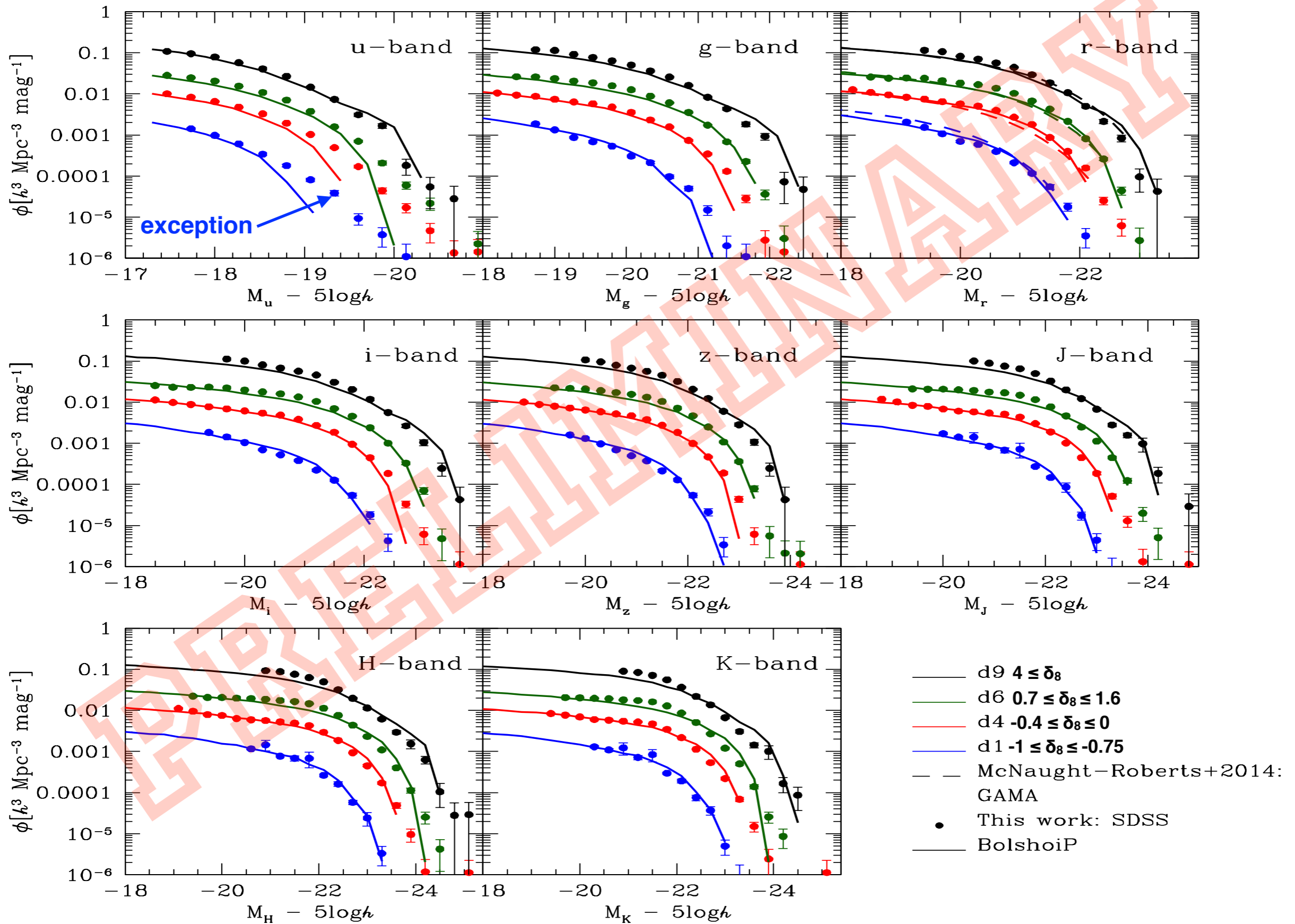
**At the same environmental density, halo properties are independent of cosmic web location.** It doesn't matter whether a halo is in a cosmic void, wall, or filament, what matters is the halos's environmental density. The properties studied are mass accretion rate, spin, halo concentration, scale factor of the last major merger, and prolateness. We had expected that a web's cosmic web location would matter for at least some of these halo properties. That it does not is a significant discovery.

GAMA data show that the galaxy luminosity function is also independent of web environment at fixed density (Eardley et al. MNRAS 2015). This contrasts with the finding that the halo mass function is dependent on web location at the same density using the v-web (Metuki, Liebeskind, Hoffman 2016).



# Abundance Matching LF and MF Are Independent of Density

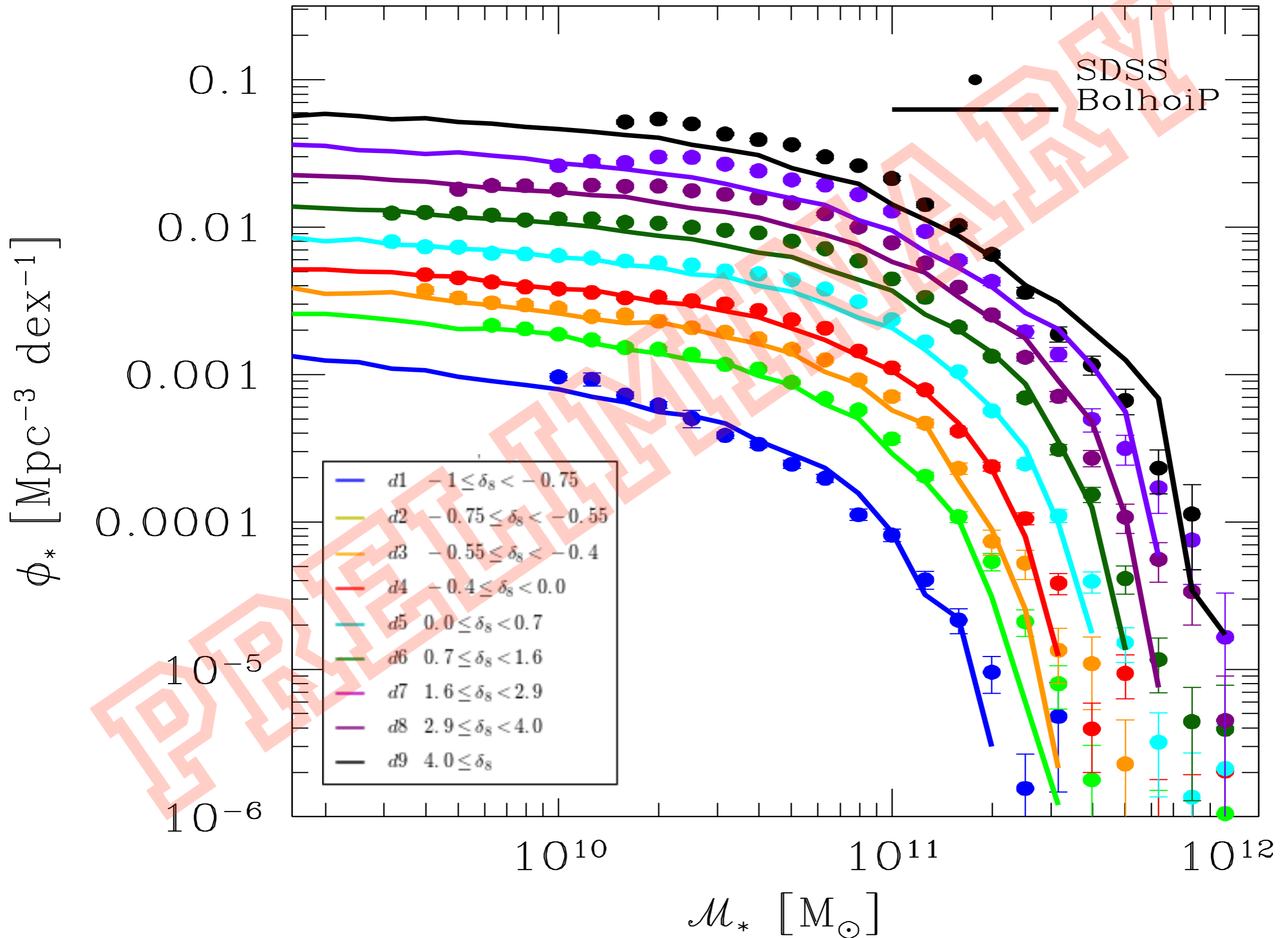
Radu Dragomir, Aldo Rodríguez-Puebla, Joel R. Primack, Christoph T. Lee, Peter Behroozi, Doug Hellinger, Avishai Dekel (in preparation)



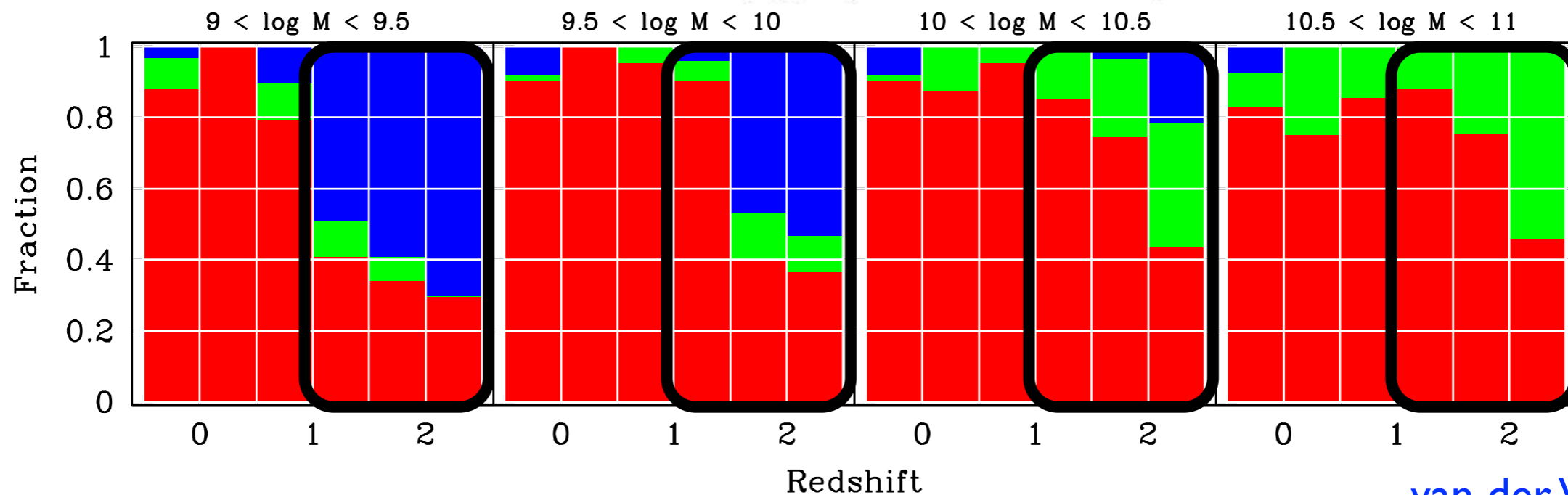
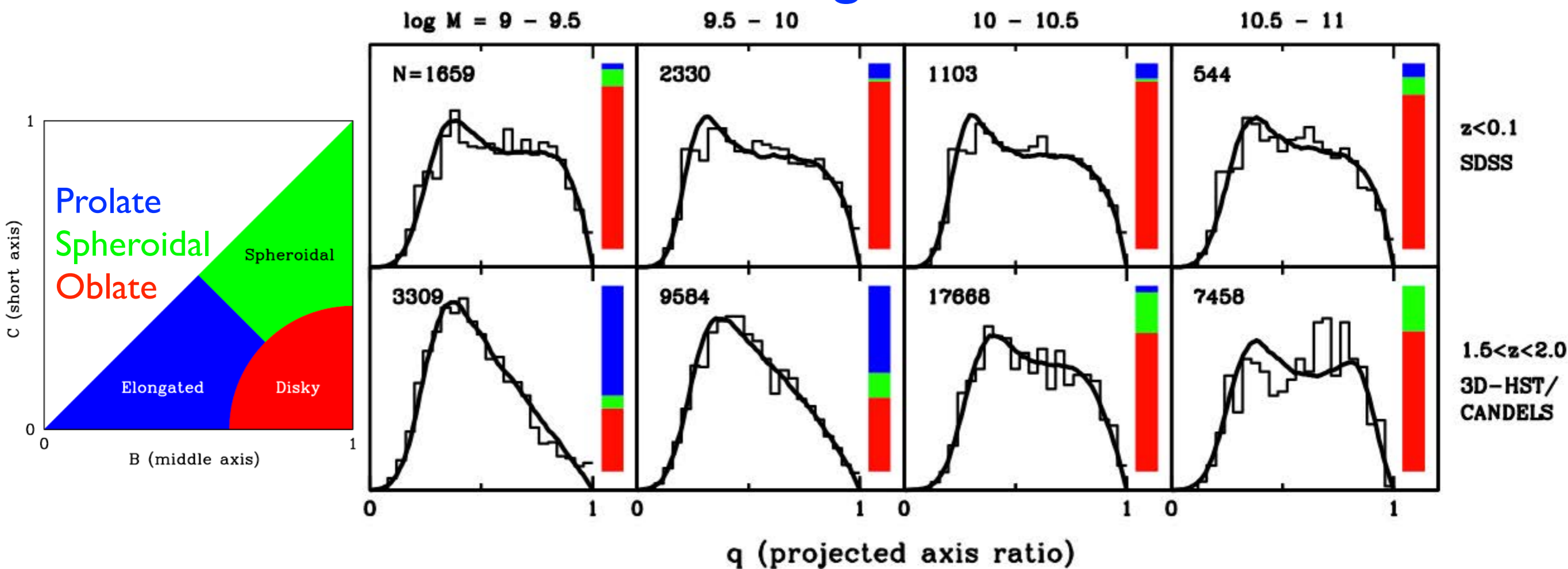


# Abundance Matching LF and MF Are Independent of Density

Radu Dragomir, Aldo Rodríguez-Puebla, Joel R. Primack, Christoph T. Lee,  
Peter Behroozi, Doug Hellinger, Avishai Dekel (in preparation)



# Prolate Galaxies Dominate at High Redshifts & Low Masses



van der Wel+2014

See also Morphological Survey of Galaxies  $z=1.5-3.6$  [Law, Steidel+ ApJ 2012](#)

When Did Round Disk Galaxies Form? [T. M. Takeuchi+ ApJ 2015](#)



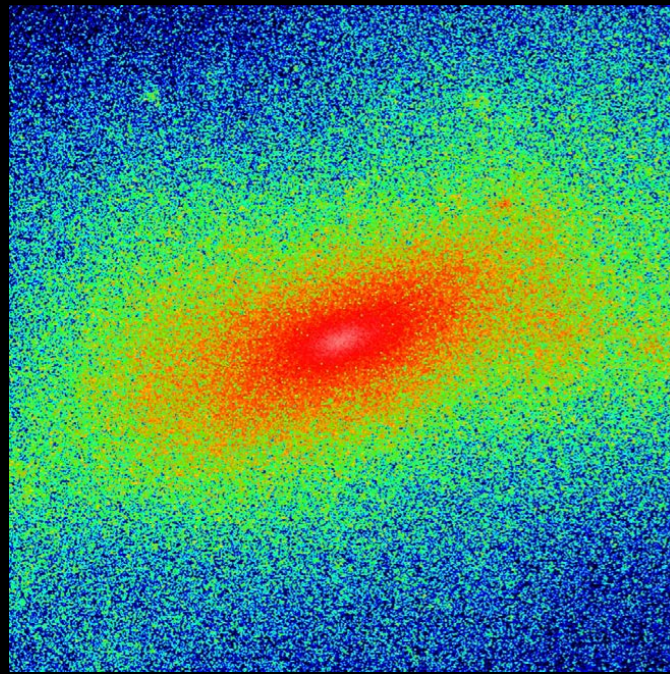
Our cosmological zoom-in simulations often produce elongated galaxies like observed ones. The elongated stellar distribution follows the elongated inner dark matter halo.

Prolate DM halo → elongated galaxy

DM

VELA28

stars



$z \approx 2$   
 $R_{\text{vir}} = 70 \text{ kpc}$   
 $M_{\text{vir}} = 2 \cdot 10^{11} M_{\odot}$   
 $M_{\text{star}} \approx 10^9 M_{\odot}$

Dark matter halos are elongated, especially near their centers. Initially stars follow the gravitationally dominant dark matter, as shown. But later as the ordinary matter central density grows and it becomes gravitationally dominant, the star and dark matter distributions both become disk-like — as observed by Hubble Space Telescope (van der Wel+ ApJL Sept 2014).

Monthly Notices

of the

ROYAL ASTRONOMICAL SOCIETY

MNRAS 453, 408–413 (2015)

## Formation of elongated galaxies with low masses at high redshift

Daniel Ceverino, Joel Primack and Avishai Dekel

### ABSTRACT

We report the identification of elongated (triaxial or prolate) galaxies in cosmological simulations at  $z \sim 2$ . These are preferentially low-mass galaxies ( $M_* \leq 10^{9.5} M_{\odot}$ ), residing in dark matter (DM) haloes with strongly elongated inner parts, a common feature of high-redshift DM haloes in the cold dark matter cosmology. A large population of elongated galaxies produces a very asymmetric distribution of projected axis ratios, as observed in high- $z$  galaxy surveys. This indicates that the majority of the galaxies at high redshifts are not discs or spheroids but rather galaxies with elongated morphologies

Nearby large galaxies are mostly disks and spheroids — but they start out looking more like pickles.

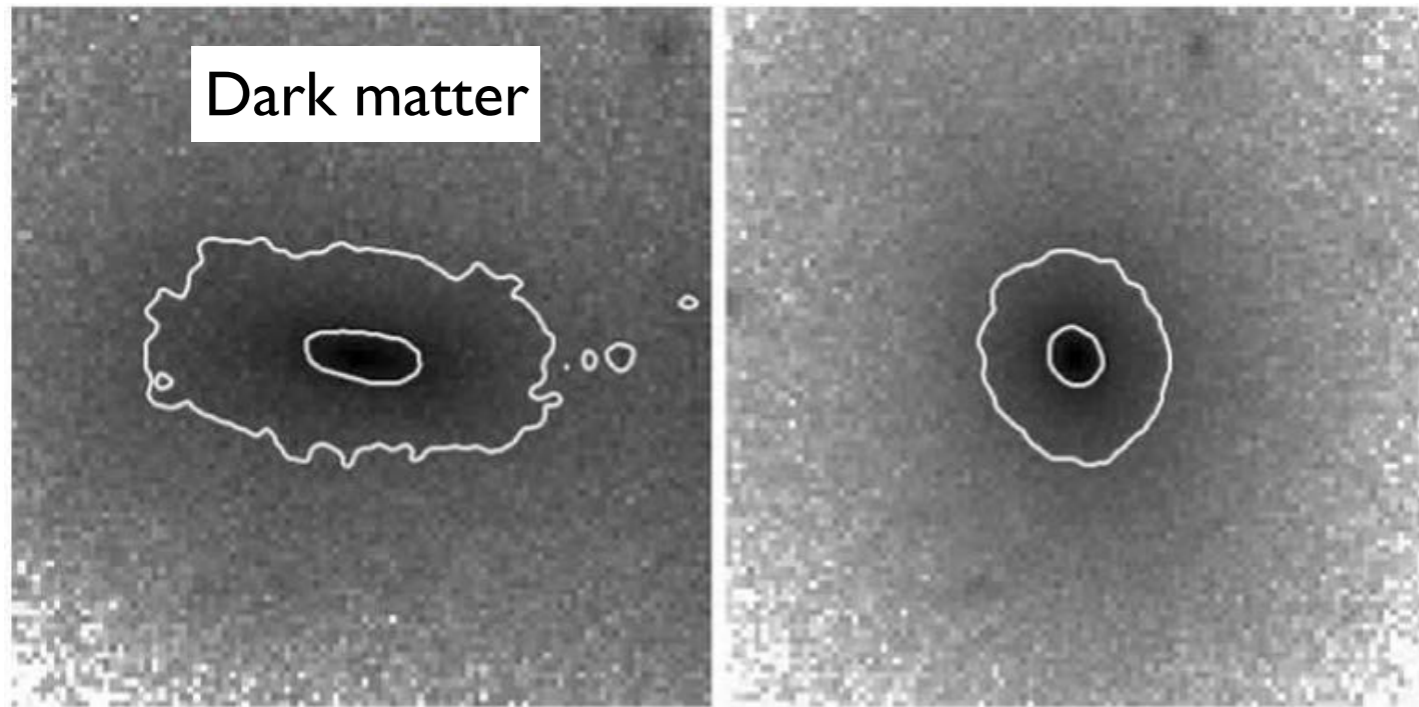
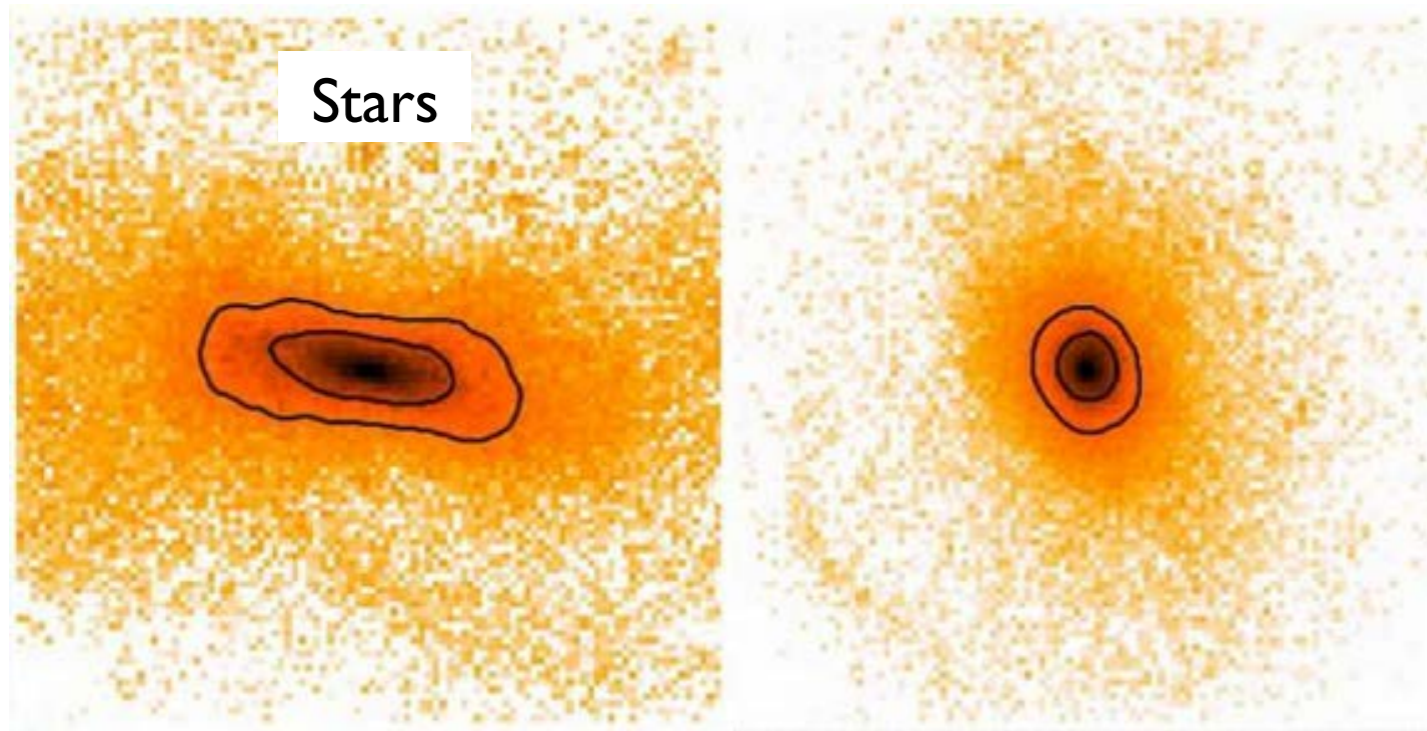




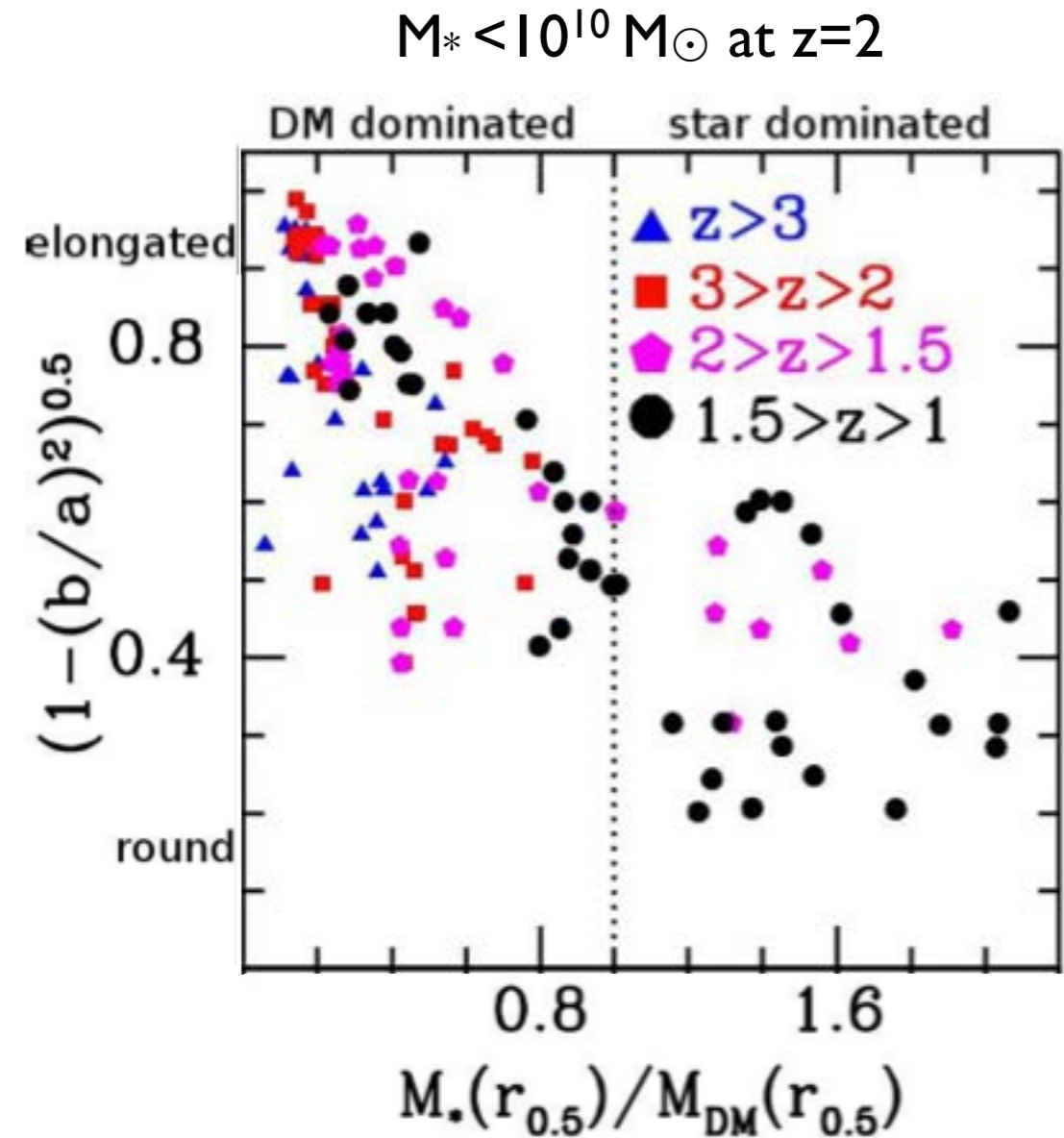
# Formation of elongated galaxies with low masses at high redshift

Daniel Ceverino, Joel Primack and Avishai Dekel

MNRAS 2015



20 kpc



Also Tomassetti et al. 2016 MNRAS

Simulated elongated galaxies are aligned with cosmic web filaments, become round after compaction (gas inflow to center)





Kavli Institute for  
Theoretical Physics  
University of California, Santa Barbara

Quantifying and Understanding the  
Galaxy — Halo Connection

May 15-19, 2017

# Structural Evolution in the Galaxy-Halo Connection, and Halo Properties as a Function of Environment Density and Web Location

Joel Primack

- **SHARC**:  $\sim 0.3$  dex dispersion in halo  $\dot{M}/M \Rightarrow$  similar dispersion in  $\dot{M}^*/M^*$  on the Main Sequence
- **Abundance matching with radii & mergers**  $\Rightarrow R^* \sim M^{*1/3}$  goes to  $R^* \sim M^{*2}$  after quenching, & **quenching downsizing**:  $\Sigma_1$  grows till quenching,  $\Sigma_{1,\text{quench}}$  larger & at higher  $z$  for higher  $M^*$
- **Galaxy 3D half-mass radii**  $R^*_{3D} \approx 0.5 \langle \lambda_{\text{Bullock}} \rangle R_{\text{halo}}$  for  $0 < z < 3$ , but  $\langle \lambda_{\text{Peebles}} \rangle \downarrow$  with  $z \uparrow$
- **Halo properties**  $\dot{M}/M$ ,  $\lambda$ ,  $C_{\text{NFW}}$ ,  $a_{\text{LMM}}$ , **shape don't depend on web location at fixed density**
- **Spin  $\lambda$  30% smaller at low density tests whether galaxy  $R^*$  is determined by host halo  $\lambda$**
- **Halo Mass Loss: Evaporation after Merger**  $\Rightarrow C_{\text{NFW}} \downarrow$  &  $\lambda \uparrow$ , **Tidal Stripping**  $\Rightarrow C_{\text{NFW}} \uparrow$  &  $\lambda \downarrow$
- **Galaxy Luminosity-Halo Mass, Stellar Mass-Halo Mass relations are independent of density**
- **Forming galaxies are elongated & oriented along filaments, become round after compaction**